BCVEGPY: An Event Generator for Hadronic Production of the B_c Meson

Chao-Hsi Chang[1,2,3] *, Chafik Driouichi[3] †, Paula Eerola[3] ‡ and Xing-Gang Wu[1§]

[1] *Institute of Theoretical Physics, Chinese Academy of Sciences, P.O.Box 2735, Beijing 100080, China.*

[2] *CCAST (World Laboratory), P.O.Box 8730, Beijing 100080, China.*¶

[3] *Experimental High Energy Physics, Department of Physics, Lund University, Box 118, SE-22100 Lund, Sweden.*

Abstract

We have written a Fortran programme BCVEGPY, which is an event generator for the hadronic production of the B_c meson through the dominant hard subprocess $gg \to B_c(B_c^*) + b + \bar{c}$. To achieve a compact programme, we have written the amplitude of the subprocess with the particle helicity technique and made it as symmetric as possible, by decomposing the gluon self couplings and then applying the symmetries. To check the programme, various cross sections of the subprocess have been computed numerically and compared with those in the literature. BCVEGPY is written in a PYTHIA-compatible format, thus it is easy to implement in PYTHIA.

PACS numbers: 13.85.Ni, 12.38.Bx, 14.40.Nd, 14.40.Lb.

Keywords: B_c meson, hadronic production, event generator.

* email: zhangzx@itp.ac.cn

† email:chafik.driouichi@hep.lu.se

‡ email:paula.eerola@hep.lu.se

§ email: xgwu@itp.ac.cn

¶ Not correspondence address.

I. INTRODUCTION

B_c-physics has been attracting an increasing attention recently, due to the experimental discovery of the B_c meson[1], and theoretical progress[2, 3, 4, 5, 6, 7, 8, 9, 10, 11, 12, 13, 14, 15, 16, 17]. Since one can collect a high-statistics sample of B_c mesons only at high energy hadronic colliders[2, 3, 5, 6, 7, 8, 9], we have re-written a generator for the hadronic production of B_c. The generator is a Fortran program package called BCVEGPY.

The hadronic production of the B_c and B_c^* mesons[28] has been estimated by the authors of Refs.[6, 10] with the fragmentation approach and by the authors of Refs.[7, 8, 9] with the so-called 'complete calculation' approach i.e. to compute the production completely at the lowest order (α_s^4) in terms of the dominant subprocess of perturbative QCD (pQCD) $gg \to B_c(B_c^*) + \bar{c} + b$. Further note that since $m_b \gg m_c \gg \Lambda_{QCD}$, apart from the fact that c and $\bar{b}$ quarks combine into $B_c(B_c^*)$ non-perturbatively, the rest of the subprocess is always 'hard' and can be well calculated with pQCD[7, 8, 9]. These two approaches have different advantages but both of them are in the framework of pQCD, and attribute the non-perturbative factor in the production to the decay constant, *i.e.* the non-relativistic wave function of the $B_c(B_c^*)$ at the origin (the former through the fragmentation function and the latter directly). Within theoretical uncertainties, the two approaches can agree numerically, especially when the component of gluon fragmentation is involved[10]. The fragmentation approach is comparatively simple and can reach to leading logarithm order (LLO) of pQCD, but is satisfied only in the case if one is only interested in the produced $B_c(B_c^*)$ itself. The complete calculation approach has the great advantage that it retains the information about the $\bar{c}$ and b quark (jets) associated with the B_c meson in the production. From the experimental point of view this is a more relevant case. Therefore, we have written the hadronic production programme for B_c mesons based on the complete calculation approach (full pQCD complete calculation at the lowest order α_s^4).

Since the non-perturbative factor in the subprocess $gg \to B_c(B_c^*) + \cdots$, i.e. the decay constant of the $B_c(B_c^*)$ meson, can be calculated by means of the potential model for heavy quark-antiquark systems[11], the estimates of the production are full theoretical predictions of pQCD without additional experimental input. In view of future experimental studies of the $B_c(B_c^*)$ after the CDF discovery (RUN-I, at Tevatron), i.e., concerning the needs of experimental feasibility studies for various topics of $B_c(B_c^*)$ meson in hadronic collisions at

Tevatron and LHC[29], we would like to write a paper on the Fortran package BCVEGPY with detailed explanation. In addition, we emphasize here that, as explained later, the present generator has been formulated in a very different way from those in Refs.[7, 8], and through carefully comparing the results obtained by BCVEGPY with those obtained in Refs.[7, 8], a solid and independent check of BCVEGPY is well made.

At LHC the beam luminosity and the production cross section (at such a high energy $\sqrt{S} = 14$TeV) are so high that the rate of producing $B_c(B_c^*)$ events can be 10^{8-9} per year. At Tevatron, although the luminosity and production cross section are lower than at LHC, the rate of producing $B_c(B_c^*)$ events still is about 10^{4-5} per year, only $3 \sim 4$ orders of magnitude lower than at LHC. The B_c meson has sizable and abundant weak decay modes relating directly to c or/and $\bar{b}$ flavor respectively, so that with so high production such as at LHC, even the detecting efficiencies being taken into account, one can reach a statistical accuracy of 10^{-2} for most of the decay modes[12, 13, 14]. Thus there is an acute need for a $B_c(B_c^*)$ event generator in order to be able to perform feasibility studies, and this is why we have written the present paper on BCVEGPY. A particularly interesting topic, which is worth noting here, is the study of $B_s - \bar{B}_s$ mixing and CP violation in B_s meson decays through $B_c(B_c^*) \to B_s \cdots$[3, 4]. The B_c meson has a very large branching ratio to decay to a B_s meson ($Br(B_c \to B_s \cdots) \simeq$ several tens percents[12, 13, 14]), and the B_s mesons obtained by such B_c decays are tagged precisely at the B_c decay vertex, if the charge of the B_c meson and/or its decay products are measured. A large-statistics sample of tagged B_s mesons at LHC, and even at Tevatron, offers a great potential for the interesting B_s physics[3].

As pointed out in Ref.[7], according to pQCD there is another production mechanism by a quark pair annihilation subprocess $q\bar{q} \to B_c(B_c^*) + \bar{c} + b$. Nevertheless, the 'luminosity' of gluons is much higher than that of quarks in pp collisions (LHC) and in $p\bar{p}$ collisions (Tevatron), and there is a suppression factor due to the virtual gluon propagator in the annihilation. Therefore the contribution from this mechanism is negligible compared to the dominant one. The calculations in Refs.[6, 8, 9, 10] neglected the contribution from the quark pair mechanism, and the BCVEGPY package follows the same approximation.

In order to make the programme very compact, we write BCVEGPY by applying the 'helicity technique' to the amplitude of the subprocess. The technique may be traced back to the work in Ref.[18]. The helicity technique has been developed by the CALKUL

collaboration[19, 20] for massless gauge theories. Further development for the massive fermion case with Abelian gauge field(s) as well as for the massless fermion case with non-Abelian gauge field(s) was done by several groups[21, 22, 23, 24]. When the helicities[30] of all the external massless particles are fixed, CALKUL calculates the 'probability rate' in the following way. First, Feynman diagrams with precise helicities for the external particles are computed one by one for the concerned process with helicity techniques, and a complex number for each Feynman diagram is obtained. Then all the obtained complex numbers are summed up. Finally the squared modulus of the summed result is taken, averaging over the helicities of the particles in initial state and summing over the helicities of the particles in final state if an unpolarized case is considered. If a polarized process is considered, one needs only to stop the calculation before averaging over the helicities of the particles in initiate state and summing over the helicities of the particles in final state.

The massless spinor technique may, in fact, be applied to the case where massive fermion(s) and non-Abelian gauge field(s) are involved in the concerned process, if a suitable 'generalization' could be done together with some further rearrangements. Our present subprocess contains non-Abelian gluons and massive fermions. Thus, in order to make use of the massless spinor technique for obtaining a compact result, we need a suitable generalization with appropriate rearrangements. We will describe the procedure here below. Our strategy for the generalization is to convert the problem into an equivalent 'massless' one and to extend the 'symmetries' as much as possible. Then we try to apply the symmetries of the converted amplitude and the helicity technique to the present problem so as to make the programme compact. According to pQCD, at order α_s^4 there are 36 Feynman diagrams for the 'hard' subprocess $gg \to B_c + \bar{c} + b$. To extend the symmetries for the amplitude corresponding to the 36 diagrams, we neither consider the color factors nor distinguish the flavors of the fermion lines at the moment. Then, these diagrams may be grouped into only a few typical ones according to the fermion lines and the structures of the contained γ-matrices on the lines in the Feynman diagrams, because of the Feynman diagram symmetries. To apply the symmetries in writing up the program, we first focus on the numerator of the amplitude related to each typical fermion line, and deal with the γ-matrices precisely. We then, having suitable four-momentum set for the numerator and denominator, respectively implement proper numerator factors for the fermion lines: color factors, suitable denominator and spinors (corresponding to the external lines) *etc*. Finally we obtain an exact and full typical

fermion line, which appears in Feynman diagrams. When all kinds of typical fermion line factors, factors for external lines of gluons and gluon propagators are 'assembled', then the full term, corresponding to the Feynman diagram of the amplitude, is achieved. The resulting program is indeed very compact and potentially reduces the execution time significantly. In general, to write an amplitude according to helicities, each massive fermion line should be decomposed into two light-like spinor lines, but this is not unique[19, 20, 21, 22, 23, 24]. Here we use the identity $\not{k} = |k+\rangle\langle k+| + |k-\rangle\langle k-|$ (k is a light-like four-momentum) to simplify the fermion (quark) lines by spinor products.

To verify that the program BCVEGPY is correct, we check it by taking the same parameters as in Ref.[8], compute the cross-section of the subprocess $gg \to B_c(B_c^*) + \bar{c} + b$ by integrating out the unobserved variables numerically, and compare the obtained results with those in Ref.[8] carefully. Since BCVEGPY is based on helicity techniques which is totally different from those in Ref.[8], the comparison is a very good check both for BCVEGPY and for that in Ref.[8].

Since the mass difference between $B_c[1,^1S_0]$ and $B_c^*[1,^3S_1]$ is small, the B_c^* decays through an electromagnetic transition (M1) $B_c^* \to B_c + \gamma$ with an almost 100% branching ratio and the photon in the decay is quite soft, so the production of B_c^* can be considered as an additional source of B_c production (with an additional soft photon). Furthermore, since $J^P = 0^-$ for B_c, the polarizations of b and/or $\bar{c}$-jets will be lost during their hadronization, so the polarization effects including those of b and/or $\bar{c}$-jets in the production of B_c are therefore not interesting, so BCVEGPY program calculates the process for the un-polarized case only, although theoretically it can work out certain polarization effects due to B^* and/or b and/or $\bar{c}$-jets.

We write the BCVEGPY package following the format of PYTHIA[25] so that the generator could be easily adapted into the PYTHIA environment. In this way our generator can be used for generating complete events. To increase the Monte Carlo simulation efficiency for high dimensional phase space integration, we set up a switch in BCVEGPY to choose if the VEGAS program for obtaining the sampling importance function is used or not. We also use several parameters, such as for the maximum differential cross sections etc, to meet the needs for the initializations of PYTHIA.

This paper is organized as follows. In Section II we show how to extend the symmetries by: focussing the γ-matrix strings of fermion lines in Feynman diagrams, disregarding color-

and numeral factors *etc*; decomposing the three- and four-gluon coupling vertices; grouping the decomposed diagrams; establishing the typical one in each group; applying the symmetries and helicity techniques to the problem. In Section III we outline the structure of BCVEGPY, explain how to use the programme and test (check) the programme as stated in the Introduction. Section IV summarizes the conclusions and future prospects. The details about the helicity functions for the amplitude, polarization vector for $B_c^*[^3S_1]$, routines and functions for the helicity amplitude are described in the Appendices.

II. THE HARD SUBPROCESS

Based on the factorization of perturbative QCD (pQCD), the hard subprocess play the key role of the B_c generator. In hadron collisions at high energies, the subprocess gluon-gluon fusion $gg \to B_c(B_c^*) + b + \bar{c}$ is the dominant one in hadronic production of $B_c(B_c^*)$ mesons[31]. In the following sub-sections, we will show how to deal with this subprocess.

A. The amplitude for $gg \to B_c(B_c^*) + b + \bar{c}$

At the lowest order α_s^4, there are totally 36 Feynman diagrams as shown in Figs. 1-5 for the gluon-gluon fusion process $gg \to B_c + b + \bar{c}$, so accordingly there are 36 terms in the production amplitude. As stated in the Introduction, we group the Feynman diagrams into five sets according to the structure of the fermion lines. Here there are five subsets as indicated in Figs. 1-5. To write the amplitude corresponding to the Feynman diagrams explicitly, let us first focus on writing the color structures of the diagrams separately. In fact there are five independent color factors, C_{1ij}, C_{2ij}, C_{3ij}, C_{4ij} and C_{5ij}, where $i, j = 1, 2, 3$ are the color indices of the quarks $\bar{c}$ and b respectively. They are

$$\begin{aligned}
C_{1ij} &= (T^c T^c T^a T^b)_{ij} = \frac{N^2-1}{2N}(T^a T^b)_{ij}\,, \\
C_{2ij} &= (T^c T^c T^b T^a)_{ij} = \frac{N^2-1}{2N}(T^b T^a)_{ij}\,, \\
C_{3ij} &= (T^c T^a T^c T^b)_{ij} = \frac{-1}{2N}(T^a T^b)_{ij}\,, \\
C_{4ij} &= (T^c T^b T^c T^a)_{ij} = \frac{-1}{2N}(T^b T^a)_{ij}\,, \\
C_{5ij} &= -\frac{1}{2}\delta_{ij} Tr[T^a T^b]\,.
\end{aligned} \tag{1}$$

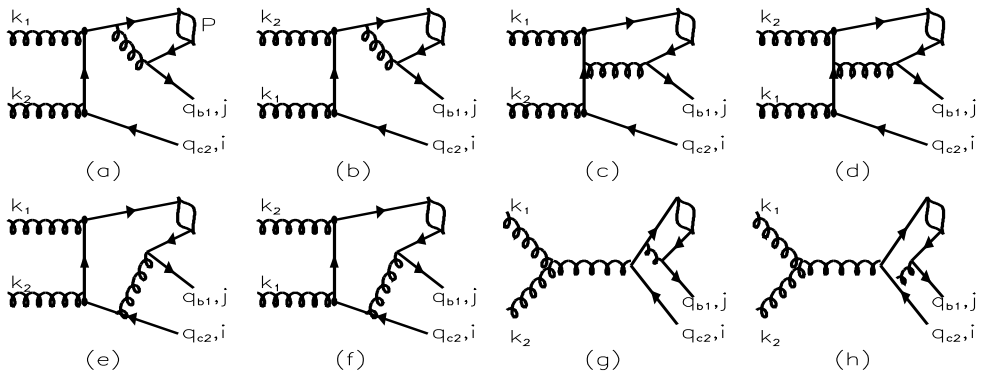

FIG. 1: Feynman diagrams that can be directly grouped into the cc subset. Here i and j are the color indices of $\bar{c}$ and b respectively.

To make the final amplitude compact, we introduce two extra color factors, C'_{5ij} and C'_{6ij}, which satisfy

$$\begin{aligned} C'_{5ij} &= C_{3ij} - C_{5ij} = (T^c T^a T^b T^c)_{ij} = \frac{1}{2}\delta_{ij} Tr[T^a T^b] - \frac{1}{2N}(T^a T^b)_{ij} \,, \\ C'_{6ij} &= C_{4ij} - C_{6ij} = (T^c T^b T^a T^c)_{ij} = \frac{1}{2}\delta_{ij} Tr[T^b T^a] - \frac{1}{2N}(T^b T^a)_{ij} \,. \end{aligned} \tag{2}$$

All the color factors in the subprocess can be expressed by the above five independent color factors, *i.e.* in the amplitude all the color factors may be written in terms of these five explicitly. To obtain the desired result, the general commutation relation for the color factors

$$[T_a, T_b] = i f_{abc} T_c \tag{3}$$

has been applied to three- or four-gluon vertice of the Feynman diagrams, where f_{abc} is the antisymmetric $SU(3)$ structure constant.

The terms of the amplitude corresponding to the grouped Feynman diagrams are written as below.

The first group, Fig.1:

$$\begin{aligned} M_{1a} &= C_{2ij}\bar{u}_s(q_{b1}) i \int \frac{d^4q}{(2\pi)^4} \left\{ \gamma_\delta \frac{\bar{\chi}_P(q)}{(q_{b1}+q_{b2})^2} \gamma_\delta \frac{\not{k}_1 + \not{k}_2 - \not{q}_{c2} + m_c}{(k_1+k_2-q_{c2})^2 - m_c^2} \not{\epsilon}_1^{\lambda_1} \cdot \right. \\ &\quad \left. \frac{\not{k}_2 - \not{q}_{c2} + m_c}{(k_2-q_{c2})^2 - m_c^2} \not{\epsilon}_2^{\lambda_2} \right\} v_{s'}(q_{c2}) \,, \\ M_{1b} &= C_{1ij}\bar{u}_s(q_{b1}) i \int \frac{d^4q}{(2\pi)^4} \left\{ \gamma_\delta \frac{\bar{\chi}_P(q)}{(q_{b1}+q_{b2})^2} \gamma_\delta \frac{\not{k}_1 + \not{k}_2 - \not{q}_{c2} + m_c}{(k_1+k_2-q_{c2})^2 - m_c^2} \not{\epsilon}_2^{\lambda_2} \cdot \right. \end{aligned}$$

$$
\begin{aligned}
& \frac{\not k_1 - \not q_{c2} + m_c}{(k_1 - q_{c2})^2 - m_c^2} \not\epsilon_1^{\lambda_1} \Big\} v_{s'}(q_{c2}) \ , \\
M_{1c} \ = \ & C_{4ij} \bar u_s(q_{b1}) i \int \frac{d^4q}{(2\pi)^4} \Big\{ \gamma_\delta \frac{\bar\chi_P(q)}{(q_{b1}+q_{b2})^2} \not\epsilon_1^{\lambda_1} \frac{\not q_{c1} - \not k_1 + m_c}{(q_{c1}-k_1)^2 - m_c^2} \gamma_\delta \cdot \\
& \frac{\not k_2 - \not q_{c2} + m_c}{(k_2 - q_{c2})^2 - m_c^2} \not\epsilon_2^{\lambda_2} \Big\} v_{s'}(q_{c2}) \ , \\
M_{1d} \ = \ & C_{3ij} \bar u_s(q_{b1}) i \int \frac{d^4q}{(2\pi)^4} \Big\{ \gamma_\delta \frac{\bar\chi_P(q)}{(q_{b1}+q_{b2})^2} \not\epsilon_2^{\lambda_2} \frac{\not q_{c1} - \not k_2 + m_c}{(q_{c1}-k_2)^2 - m_c^2} \gamma_\delta \cdot \\
& \frac{\not k_1 - \not q_{c2} + m_c}{(k_1 - q_{c2})^2 - m_c^2} \not\epsilon_1^{\lambda_1} \Big\} v_{s'}(q_{c2}) \ , \\
M_{1e} \ = \ & C'_{6ij} \bar u_s(q_{b1}) i \int \frac{d^4q}{(2\pi)^4} \Big\{ \gamma_\delta \frac{\bar\chi_P(q)}{(q_{b1}+q_{b2})^2} \not\epsilon_1^{\lambda_1} \frac{\not q_{c1} - \not k_1 + m_c}{(q_{c1}-k_1)^2 - m_c^2} \not\epsilon_2^{\lambda_2} \cdot \\
& \frac{\not q_{c1} - \not k_1 - \not k_2 + m_c}{(q_{c1}-k_1-k_2)^2 - m_c^2} \gamma_\delta \Big\} v_{s'}(q_{c2}) \ , \\
M_{1f} \ = \ & C'_{5ij} \bar u_s(q_{b1}) i \int \frac{d^4q}{(2\pi)^4} \Big\{ \gamma_\delta \frac{\bar\chi_P(q)}{(q_{b1}+q_{b2})^2} \not\epsilon_2^{\lambda_2} \frac{\not q_{c1} - \not k_2 + m_c}{(q_{c1}-k_2)^2 - m_c^2} \not\epsilon_1^{\lambda_1} \cdot \\
& \frac{\not q_{c1} - \not k_1 - \not k_2 + m_c}{(q_{c1}-k_1-k_2)^2 - m_c^2} \gamma_\delta \Big\} v_{s'}(q_{c2}) \ , \\
M_{1g} \ = \ & (C_{2ij} - C_{1ij}) \bar u_s(q_{b1}) i \int \frac{d^4q}{(2\pi)^4} \Big\{ \gamma_\delta \frac{\bar\chi_P(q)}{(q_{b1}+q_{b2})^2} \gamma_\delta \frac{\not k_1 + \not k_2 - \not q_{c2} + m_c}{(k_1+k_2-q_{c2})^2 - m_c^2} \cdot \\
& \frac{\gamma_\alpha \epsilon_{1\mu}^{\lambda_1} \epsilon_{2\nu}^{\lambda_2}}{(k_1+k_2)^2} \Big((k_1-k_2)_\alpha g_{\mu\nu} + (2k_2+k_1)_\mu g_{\nu\alpha} + (-2k_1-k_2)_\nu g_{\mu\alpha} \Big) \Big\} v_{s'}(q_{c2}) \ , \\
M_{1h} \ = \ & (C'_{6ij} - C'_{5ij}) \bar u_s(q_{b1}) i \int \frac{d^4q}{(2\pi)^4} \Big\{ \gamma_\delta \frac{\bar\chi_P(q)}{(q_{b1}+q_{b2})^2} \frac{\gamma_\alpha \epsilon_{1\mu}^{\lambda_1} \epsilon_{2\nu}^{\lambda_2}}{(k_1+k_2)^2} \frac{\not q_{c1} - \not k_1 - \not k_2 + m_c}{(k_1+k_2-q_{c1})^2 - m_c^2} \cdot \\
& \gamma_\delta \Big((k_1-k_2)_\alpha g_{\mu\nu} + (2k_2+k_1)_\mu g_{\nu\alpha} + (-2k_1-k_2)_\nu g_{\mu\alpha} \Big) \Big\} v_{s'}(q_{c2}) \ .
\end{aligned}
\tag{4}
$$

The second group, Fig.2:

$$
\begin{aligned}
M_{2a} \ = \ & (C'_{6ij}) \bar u_s(q_{b1}) i \int \frac{d^4q}{(2\pi)^4} \Big\{ \gamma_\delta \frac{\not k_1 + \not k_2 - \not q_{b2} + m_b}{(k_1+k_2-q_{b2})^2 - m_b^2} \not\epsilon_1^{\lambda_1} \frac{\not k_2 - \not q_{b2} + m_b}{(k_2-q_{b2})^2 - m_b^2} \not\epsilon_2^{\lambda_2} \cdot \\
& \frac{\bar\chi_P(q)}{(q_{c1}+q_{c2})^2} \gamma_\delta \Big\} v_{s'}(q_{c2}) \ , \\
M_{2b} \ = \ & (C'_{5ij}) \bar u_s(q_{b1}) i \int \frac{d^4q}{(2\pi)^4} \Big\{ \gamma_\delta \frac{\not k_1 + \not k_2 - \not q_{b2} + m_b}{(k_1+k_2-q_{b2})^2 - m_b^2} \not\epsilon_2^{\lambda_2} \frac{\not k_1 - \not q_{b2} + m_b}{(k_1-q_{b2})^2 - m_b^2} \not\epsilon_1^{\lambda_1} \cdot \\
& \frac{\bar\chi_P(q)}{(q_{c1}+q_{c2})^2} \gamma_\delta \Big\} v_{s'}(q_{c2}) \ , \\
M_{2c} \ = \ & (C_{4ij}) \bar u_s(q_{b1}) i \int \frac{d^4q}{(2\pi)^4} \Big\{ \not\epsilon_1^{\lambda_1} \frac{\not q_{b1} - \not k_1 + m_b}{(q_{b1}-k_1)^2 - m_b^2} \gamma_\delta \frac{\not k_2 - \not q_{b2} + m_b}{(k_2-q_{b2})^2 - m_b^2} \not\epsilon_2^{\lambda_2} \cdot
\end{aligned}
$$

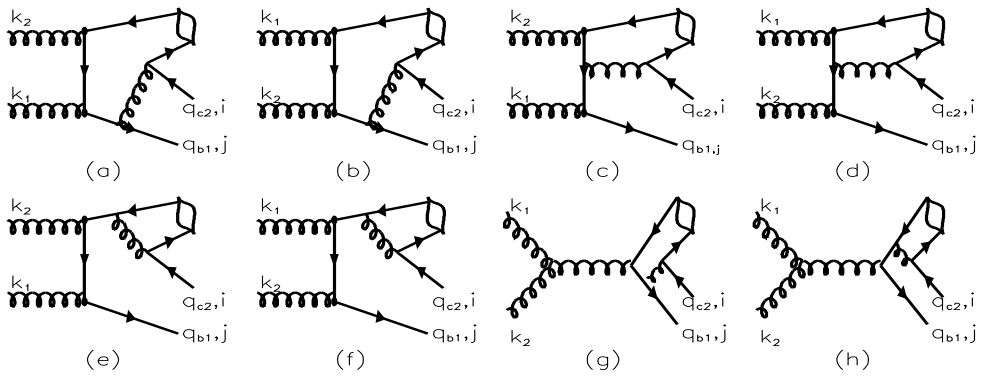

FIG. 2: Feynman diagrams that can be directly grouped into the $b\bar{b}$ subset. Here i and j are the color indices of $\bar{c}$ and b respectively.

$$
\begin{aligned}
& \frac{\bar{\chi}_P(q)}{(q_{c1}+q_{c2})^2}\gamma_\delta\Big\} v_{s'}(q_{c2}) \ , \\
M_{2d} &= (C_{3ij})\bar{u}_s(q_{b1})i\int\frac{d^4q}{(2\pi)^4}\Big\{\not\epsilon_2^{\lambda_2}\frac{\not q_{b1}-\not k_2+m_b}{(q_{b1}-k_2)^2-m_b^2}\gamma_\delta\frac{\not k_1-\not q_{b2}+m_b}{(k_1-q_{b2})^2-m_b^2}\not\epsilon_1^{\lambda_1}\cdot \\
& \frac{\bar{\chi}_P(q)}{(q_{c1}+q_{c2})^2}\gamma_\delta\Big\} v_{s'}(q_{c2}) \ , \\
M_{2e} &= (C_{2ij})\bar{u}_s(q_{b1})i\int\frac{d^4q}{(2\pi)^4}\Big\{\not\epsilon_1^{\lambda_1}\frac{\not q_{b1}-\not k_1+m_b}{(q_{b1}-k_1)^2-m_b^2}\not\epsilon_2^{\lambda_2}\frac{\not q_{b1}-\not k_1-\not k_2+m_b}{(q_{b1}-k_1-k_2)^2-m_b^2}\gamma_\delta\cdot \\
& \frac{\bar{\chi}_P(q)}{(q_{c1}+q_{c2})^2}\gamma_\delta\Big\} v_{s'}(q_{c2}) \ , \\
M_{2f} &= (C_{1ij})\bar{u}_s(q_{b1})i\int\frac{d^4q}{(2\pi)^4}\Big\{\not\epsilon_2^{\lambda_2}\frac{\not q_{b1}-\not k_2+m_b}{(q_{b1}-k_2)^2-m_b^2}\not\epsilon_1^{\lambda_1}\frac{\not q_{b1}-\not k_1-\not k_2+m_b}{(q_{b1}-k_1-k_2)^2-m_b^2}\gamma_\delta\cdot \\
& \frac{\bar{\chi}_P(q)}{(q_{c1}+q_{c2})^2}\gamma_\delta\Big\} v_{s'}(q_{c2}) \ , \\
M_{2g} &= (C'_{6ij}-C'_{5ij})\bar{u}_s(q_{b1})i\int\frac{d^4q}{(2\pi)^4}\Big\{\gamma_\delta\frac{\not k_1+\not k_2-\not q_{b2}+m_b}{(k_1+k_2-q_{b2})^2-m_b^2}\frac{\gamma_\alpha\epsilon_{1\mu}^{\lambda_1}\epsilon_{2\nu}^{\lambda_2}}{(k_1+k_2)^2}\ \cdot \\
& \Big((k_1-k_2)_\alpha g_{\mu\nu}+(2k_2+k_1)_\mu g_{\nu\alpha}+(-2k_1-k_2)_\nu g_{\mu\alpha}\Big)\frac{\bar{\chi}_P(q)}{(q_{c1}+q_{c2})^2}\gamma_\delta\Big\}v_{s'}(q_{c2}) \ , \\
M_{2h} &= (C_{2ij}-C_{1ij})\bar{u}_s(q_{b1})i\int\frac{d^4q}{(2\pi)^4}\Big\{\frac{\gamma_\alpha\epsilon_{1\mu}^{\lambda_1}\epsilon_{2\nu}^{\lambda_2}}{(k_1+k_2)^2}\frac{\not q_{b1}-\not k_1-\not k_2+m_b}{(k_1+k_2-q_{b1})^2-m_b^2}\gamma_\delta\ \cdot \\
& \frac{\bar{\chi}_P(q)}{(q_{c1}+q_{c2})^2}\gamma_\delta\Big((k_1-k_2)_\alpha g_{\mu\nu}+(2k_2+k_1)_\mu g_{\nu\alpha}+(-2k_1-k_2)g_{\mu\alpha}\Big)\Big\}v_{s'}(q_{c2})\,. \qquad (5)
\end{aligned}
$$

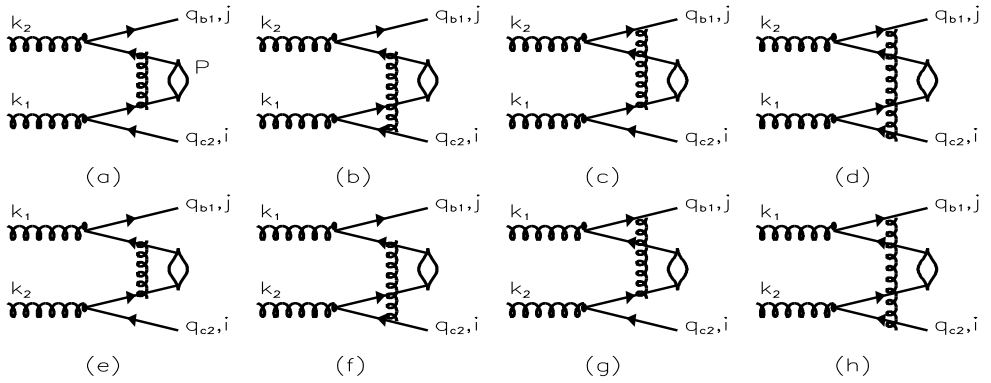

FIG. 3: Feynman diagrams that can be directly grouped into the *cb* or *bc* subsets, where the first four diagrams belong to the cb subset, while the last four belong to the bc subset. Here i and j are the color indices of $\bar{c}$ and b respectively.

The third group, Fig.3:

$$
\begin{aligned}
M_{3a} &= C_{1ij}\bar{u}_s(q_{b1})\not\epsilon_2^{\lambda_2}\frac{\not q_{b1}-\not k_2+m_b}{(q_{b1}-k_2)^2-m_b^2}i\int\frac{d^4q}{(2\pi)^4}\gamma_\delta\frac{\bar\chi_P(q)}{(k_1-q_{c1}-q_{c2})^2}\gamma_\delta\frac{\not k_1-\not q_{c2}+m_c}{(k_1-q_{c2})^2-m_c^2}\cdot\\
&\quad \not\epsilon_1^{\lambda_1}v_{s'}(q_{c2})\ ,\\
M_{3b} &= C_{3ij}\bar{u}_s(q_{b1})\not\epsilon_2^{\lambda_2}\frac{\not q_{b1}-\not k_2+m_b}{(q_{b1}-k_2)^2-m_b^2}i\int\frac{d^4q}{(2\pi)^4}\gamma_\delta\frac{\bar\chi_P(q)}{(k_1-q_{c1}-q_{c2})^2}\not\epsilon_1^{\lambda_1}\frac{\not q_{c1}-\not k_1+m_c}{(q_{c1}-k_1)^2-m_c^2}\cdot\\
&\quad \gamma_\delta v_{s'}(q_{c2})\ ,\\
M_{3c} &= C_{3ij}\bar{u}_s(q_{b1})i\int\frac{d^4q}{(2\pi)^4}\gamma_\delta\frac{\not k_2-\not q_{b2}+m_b}{(k_2-q_{b2})^2-m_b^2}\not\epsilon_2^{\lambda_2}\frac{\bar\chi_P(q)}{(k_1-q_{c1}-q_{c2})^2}\gamma_\delta\frac{\not k_1-\not q_{c2}+m_c}{(k_1-q_{c2})^2-m_c^2}\cdot\\
&\quad \not\epsilon_1^{\lambda_1}v_{s'}(q_{c2})\ ,\\
M_{3d} &= C'_{5ij}\bar{u}_s(q_{b1})i\int\frac{d^4q}{(2\pi)^4}\gamma_\delta\frac{\not k_2-\not q_{b2}+m_b}{(k_2-q_{b2})^2-m_b^2}\not\epsilon_2^{\lambda_2}\frac{\bar\chi_P(q)}{(k_1-q_{c1}-q_{c2})^2}\not\epsilon_1^{\lambda_1}\frac{\not q_{c1}-\not k_1+m_c}{(q_{c1}-k_1)^2-m_c^2}\cdot\\
&\quad \gamma_\delta v_{s'}(q_{c2})\ ,\\
M_{3e} &= C_{2ij}\bar{u}_s(q_{b1})\not\epsilon_1^{\lambda_1}\frac{\not q_{b1}-\not k_1+m_b}{(q_{b1}-k_1)^2-m_b^2}i\int\frac{d^4q}{(2\pi)^4}\gamma_\delta\frac{\bar\chi_P(q)}{(k_2-q_{c1}-q_{c2})^2}\gamma_\delta\frac{\not k_2-\not q_{c2}+m_c}{(k_2-q_{c2})^2-m_c^2}\cdot\\
&\quad \not\epsilon_2^{\lambda_2}v_{s'}(q_{c2})\ ,\\
M_{3f} &= C_{4ij}\bar{u}_s(q_{b1})\not\epsilon_1^{\lambda_1}\frac{\not q_{b1}-\not k_1+m_b}{(q_{b1}-k_1)^2-m_b^2}i\int\frac{d^4q}{(2\pi)^4}\gamma_\delta\frac{\bar\chi_P(q)}{(k_2-q_{c1}-q_{c2})^2}\not\epsilon_2^{\lambda_2}\frac{\not q_{c1}-\not k_2+m_c}{(q_{c1}-k_2)^2-m_c^2}\cdot\\
&\quad \gamma_\delta v_{s'}(q_{c2})\ ,\\
M_{3g} &= C_{4ij}\bar{u}_s(q_{b1})i\int\frac{d^4q}{(2\pi)^4}\gamma_\delta\frac{\not k_1-\not q_{b2}+m_b}{(k_1-q_{b2})^2-m_b^2}\not\epsilon_1^{\lambda_1}\frac{\bar\chi_P(q)}{(k_2-q_{c1}-q_{c2})^2}\gamma_\delta\frac{\not k_2-\not q_{c2}+m_c}{(k_2-q_{c2})^2-m_c^2}\cdot\\
&\quad \not\epsilon_2^{\lambda_2}v_{s'}(q_{c2})\ ,\\
M_{3h} &= C'_{6ij}\bar{u}_s(q_{b1})i\int\frac{d^4q}{(2\pi)^4}\gamma_\delta\frac{\not k_1-\not q_{b2}+m_b}{(k_1-q_{b2})^2-m_b^2}\not\epsilon_1^{\lambda_1}\frac{\bar\chi_P(q)}{(k_2-q_{c1}-q_{c2})^2}\not\epsilon_2^{\lambda_2}\frac{\not q_{c1}-\not k_2+m_c}{(q_{c1}-k_2)^2-m_c^2}\cdot
\end{aligned}
$$

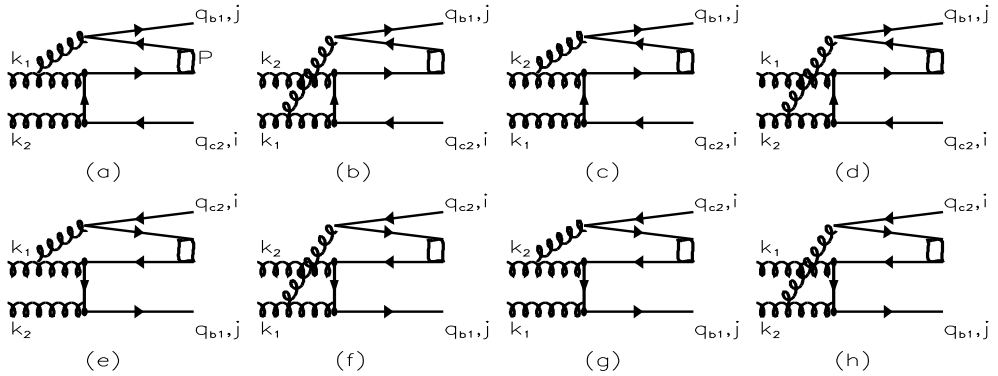

FIG. 4: Feynman diagrams with only one three-gluon vertex, which can not be directly grouped into the cc, bb, cb and bc subsets. Here i and j are the color indices of $\bar{c}$ and b respectively.

$$\gamma_\delta v_{s'}(q_{c2}) \ . \tag{6}$$

The fourth group, Fig.4:

$$\begin{aligned}
M_{4a} &= (C_{4ij}-C_{2ij})\bar{u}_s(q_{b1})i\int\frac{d^4q}{(2\pi)^4}\gamma_\delta\frac{\bar{\chi}_P(q)}{(q_{b1}+q_{b2})^2}\frac{\gamma_\alpha\epsilon_{1\mu}^{\lambda_1}}{(k_1-q_{b1}-q_{b2})^2}\Big((k_1+q_{b1}+q_{b2})_\alpha g_{\mu\delta}+\\
&\quad (k_1-2q_{b1}-2q_{b2})_\mu g_{\alpha\delta}+(q_{b1}+q_{b2}-2k_1)_\delta g_{\mu\alpha}\Big)\frac{\not k_2-\not q_{c2}+m_c}{(k_2-q_{c2})^2-m_c^2}\not\epsilon_2^{\lambda_2}v_{s'}(q_{c2})\ ,\\
M_{4b} &= (-C_{5ij})\bar{u}_s(q_{b1})i\int\frac{d^4q}{(2\pi)^4}\gamma_\delta\frac{\bar{\chi}_P(q)}{(q_{b1}+q_{b2})^2}\not\epsilon_2^{\lambda_2}\frac{\not q_{c1}-\not k_2+m_c}{(q_{c1}-k_2)^2-m_c^2}\frac{\gamma_\alpha\epsilon_{1\mu}^{\lambda_1}}{(k_1-q_{b1}-q_{b2})^2}\cdot\\
&\quad \Big((k_1+q_{b1}+q_{b2})_\alpha g_{\mu\delta}+(k_1-2q_{b1}-2q_{b2})_\mu g_{\alpha\delta}+(q_{b1}+q_{b2}-2k_1)_\delta g_{\mu\alpha}\Big)v_{s'}(q_{c2})\ ,\\
M_{4c} &= (C_{3ij}-C_{1ij})\bar{u}_s(q_{b1})i\int\frac{d^4q}{(2\pi)^4}\gamma_\delta\frac{\bar{\chi}_P(q)}{(q_{b1}+q_{b2})^2}\frac{\gamma_\alpha\epsilon_{2\mu}^{\lambda_2}}{(k_2-q_{b1}-q_{b2})^2}\Big((k_2+q_{b1}+q_{b2})_\alpha g_{\mu\delta}+\\
&\quad (k_2-2q_{b1}-2q_{b2})_\mu g_{\alpha\delta}+(q_{b1}+q_{b2}-2k_2)_\delta g_{\mu\alpha}\Big)\frac{\not k_1-\not q_{c2}+m_c}{(k_1-q_{c2})^2-m_c^2}\not\epsilon_1^{\lambda_1}v_{s'}(q_{c2})\ ,\\
M_{4d} &= (-C_{5ij})\bar{u}_s(q_{b1})i\int\frac{d^4q}{(2\pi)^4}\gamma_\delta\frac{\bar{\chi}_P(q)}{(q_{b1}+q_{b2})^2}\not\epsilon_1^{\lambda_1}\frac{\not q_{c1}-\not k_1+m_c}{(q_{c1}-k_1)^2-m_c^2}\frac{\gamma_\alpha\epsilon_{2\mu}^{\lambda_2}}{(k_2-q_{b1}-q_{b2})^2}\cdot\\
&\quad \Big((k_2+q_{b1}+q_{b2})_\alpha g_{\mu\delta}+(k_2-2q_{b1}-2q_{b2})_\mu g_{\alpha\delta}+(q_{b1}+q_{b2}-2k_2)_\delta g_{\mu\alpha}\Big)v_{s'}(q_{c2})\ ,\\
M_{4e} &= (C_{1ij}-C_{3ij})\bar{u}_s(q_{b1})i\int\frac{d^4q}{(2\pi)^4}\not\epsilon_2^{\lambda_2}\frac{\not q_{b1}-\not k_2+m_b}{(q_{b1}-k_2)^2-m_b^2}\frac{\gamma_\alpha\epsilon_{1\mu}^{\lambda_1}}{(k_1-q_{c1}-q_{c2})^2}\frac{\bar{\chi}_P(q)}{(q_{c1}+q_{c2})^2}\gamma_\delta\cdot\\
&\quad \Big((k_1+q_{c1}+q_{c2})_\alpha g_{\mu\delta}+(k_1-2q_{c1}-2q_{c2})_\mu g_{\alpha\delta}+(q_{c1}+q_{c2}-2k_1)_\delta g_{\mu\alpha}\Big)v_{s'}(q_{c2})\ ,\\
M_{4f} &= (C_{5ij})\bar{u}_s(q_{b1})i\int\frac{d^4q}{(2\pi)^4}\frac{\gamma_\alpha\epsilon_{1\mu}^{\lambda_1}}{(k_1-q_{c1}-q_{c2})^2}\frac{\not k_2-\not q_{b2}+m_b}{(k_2-q_{b2})^2-m_b^2}\not\epsilon_2^{\lambda_2}\frac{\bar{\chi}_P(q)}{(q_{c1}+q_{c2})^2}\gamma_\delta\cdot\\
&\quad \Big((k_1+q_{c1}+q_{c2})_\alpha g_{\mu\delta}+(k_1-2q_{c1}-2q_{c2})_\mu g_{\alpha\delta}+(q_{c1}+q_{c2}-2k_1)_\delta g_{\mu\alpha}\Big)v_{s'}(q_{c2})\ ,
\end{aligned}$$

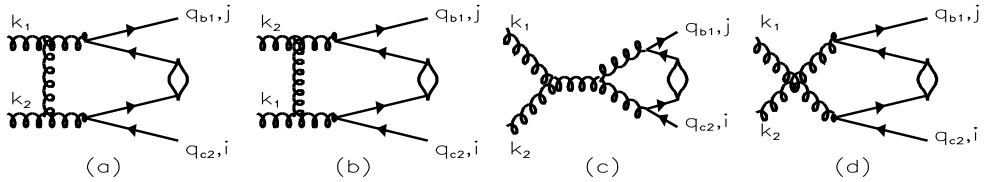

FIG. 5: Feynman diagrams with two three-gluon vertices or with a four-gluon vertex, which can not be directly grouped into the cc, bb, cb and bc subsets. Here i and j are the color indices of $\bar{c}$ and b respectively.

$$
\begin{aligned}
M_{4g} &= (C_{2ij}-C_{4ij})\bar{u}_s(q_{b1})i\int\frac{d^4q}{(2\pi)^4}\not{\epsilon}_1^{\lambda_1}\frac{\not{q}_{b1}-\not{k}_1+m_b}{(q_{b1}-k_1)^2-m_b^2}\frac{\gamma_\alpha\epsilon_{2\mu}^{\lambda_2}}{(k_2-q_{c1}-q_{c2})^2}\frac{\bar{\chi}_P(q)}{(q_{c1}+q_{c2})^2}\gamma_\delta\cdot\\
&\Big((k_2+q_{c1}+q_{c2})_\alpha g_{\mu\delta}+(k_2-2q_{c1}-2q_{c2})_\mu g_{\alpha\delta}+(q_{c1}+q_{c2}-2k_2)_\delta g_{\mu\alpha}\Big)v_{s'}(q_{c2})\ ,\\
M_{4h} &= (C_{5ij})\bar{u}_s(q_{b1})i\int\frac{d^4q}{(2\pi)^4}\frac{\gamma_\alpha\epsilon_{2\mu}^{\lambda_2}}{(k_2-q_{c1}-q_{c2})^2}\frac{\not{k}_1-\not{q}_{b2}+m_b}{(k_1-q_{b2})^2-m_b^2}\not{\epsilon}_1^{\lambda_1}\frac{\bar{\chi}_P(q)}{(q_{c1}+q_{c2})^2}\gamma_\delta\cdot\\
&\Big((k_2+q_{c1}+q_{c2})_\alpha g_{\mu\delta}+(k_2-2q_{c1}-2q_{c2})_\mu g_{\alpha\delta}+(q_{c1}+q_{c2}-2k_2)_\delta g_{\mu\alpha}\Big)v_{s'}(q_{c2})\ . \qquad (7)
\end{aligned}
$$

The fifth group Fig.5:

$$
\begin{aligned}
M_{5a} &= (C_{2ij}-C_{4ij}-C_{5ij})\bar{u}_s(q_{b1})i\int\frac{d^4q}{(2\pi)^4}\frac{\gamma_\alpha\epsilon_{1\mu}^{\lambda_1}}{(q_{b1}+q_{b2})^2}\frac{\bar{\chi}_P(q)}{(k_2-q_{c1}-q_{c2})^2}\frac{\gamma_\beta\epsilon_{2\nu}^{\lambda_2}}{(q_{c1}+q_{c2})^2}\cdot\\
&\Big((2k_1-q_{b1}-q_{b2})_\alpha g_{\mu\delta}+(2q_{b1}+2q_{b2}-k_1)_\mu g_{\alpha\delta}+(-q_{b1}-q_{b2}-k_1)_\delta g_{\mu\alpha}\Big)\cdot\\
&\Big((k_2+q_{c1}+q_{c2})_\delta g_{\nu\beta}+(k_2-2q_{c1}-2q_{c2})_\nu g_{\beta\delta}+(-2k_2+q_{c1}+q_{c2})_\beta g_{\delta\nu}\Big)v_{s'}(q_{c2})\ ,\\
M_{5b} &= (C_{1ij}-C_{3ij}-C_{5ij})\bar{u}_s(q_{b1})i\int\frac{d^4q}{(2\pi)^4}\frac{\gamma_\alpha\epsilon_{2\mu}^{\lambda_2}}{(q_{b1}+q_{b2})^2}\frac{\bar{\chi}_P(q)}{(k_1-q_{c1}-q_{c2})^2}\frac{\gamma_\beta\epsilon_{1\nu}^{\lambda_1}}{(q_{c1}+q_{c2})^2}\cdot\\
&\Big((2k_2-q_{b1}-q_{b2})_\alpha g_{\mu\delta}+(2q_{b1}+2q_{b2}-k_2)_\mu g_{\alpha\delta}+(-q_{b1}-q_{b2}-k_2)_\delta g_{\mu\alpha}\Big)\cdot\\
&\Big((k_1+q_{c1}+q_{c2})_\delta g_{\nu\beta}+(k_1-2q_{c1}-2q_{c2})_\nu g_{\beta\delta}+(-2k_1+q_{c1}+q_{c2})_\beta g_{\delta\nu}\Big)v_{s'}(q_{c2})\ ,\\
M_{5c} &= (C_{1ij}+C_{4ij}-C_{3ij}-C_{2ij})\bar{u}_s(q_{b1})i\int\frac{d^4q}{(2\pi)^4}\frac{\gamma_\alpha\epsilon_{1\mu}^{\lambda_1}}{(q_{b1}+q_{b2})^2}\frac{\bar{\chi}_P(q)}{(k_1+k_2)^2}\frac{\gamma_\beta\epsilon_{2\nu}^{\lambda_2}}{(q_{c1}+q_{c2})^2}\cdot\\
&\Big((k_1+k_2+q_{b1}+q_{b2})_\beta g_{\alpha\delta}+(k_1+k_2-2q_{b1}-2q_{b2})_\delta g_{\alpha\beta}+(q_{b1}+q_{b2}-2k_1-2k_2)_\alpha g_{\beta\delta}\Big)\cdot\\
&\Big((k_1-k_2)_\delta g_{\nu\mu}+(2k_2+k_1)_\mu g_{\nu\delta}+(-2k_1-k_2)_\nu g_{\delta\mu}\Big)v_{s'}(q_{c2})\ ,
\end{aligned}
$$

$$M_{5d} = \bar{u}_s(q_{b1})i\int\frac{d^4q}{(2\pi)^4}\frac{\gamma_\alpha\epsilon_{1\mu}^{\lambda_1}}{(q_{b1}+q_{b2})^2}\bar{\chi}_P(q)\frac{\gamma_\beta\epsilon_{2\nu}^{\lambda_2}}{(q_{c1}+q_{c2})^2}\cdot$$
$$\Big((C_{2ij}+C_{3ij}-C_{1ij}-C_{4ij})(g_{\mu\beta}g_{\nu\alpha}-g_{\mu\alpha}g_{\nu\beta})+(C_{5ij}-C_{1ij}+C_{3ij})\cdot$$
$$(g_{\mu\nu}g_{\beta\alpha}-g_{\mu\alpha}g_{\nu\beta})+(C_{5ij}-C_{2ij}+C_{4ij})(g_{\mu\nu}g_{\alpha\beta}-g_{\mu\beta}g_{\nu\alpha})\Big)v_{s'}(q_{c2})\,. \quad (8)$$

In Eqs. (4-8), k_1, k_2 and ϵ_1, ϵ_2 are the momenta and the polarization vectors of the gluons; q_{c1}, q_{b1} are the momenta of c and b quarks and q_{c2}, q_{b2} are the momenta of $\bar{c}$ and $\bar{b}$ anti-quarks, respectively. Note that in all the above equations we have omitted the factor g_s^4 (the fourth power of the QCD coupling constant), so we should consider it when evaluating the final result. For convenience, we group the terms (Feynman diagrams) according to the character of the gluon attachment to the fermion lines. The details will be explained in the next sections.

Under the non-relativistic approximation, for the weak binding system of $(c\bar{b})$ we have

$$M_{B_c} = M_{B_c^*} = M \simeq m_b + m_c\,, \quad q_{c1} = \frac{m_c}{M}P\,, \quad q_{b2} = \frac{m_b}{M}P\,, \quad (9)$$

and the wave function $\bar{\chi}_P(q)$ can be written as

$$\bar{\chi}_P(q) = \phi(q)\frac{1}{2\sqrt{M}}(\alpha\gamma_5 + \beta\not{\epsilon}(s_z))(\not{P}+M)\,, \quad (10)$$

where $\alpha = 1$, $\beta = 0$ for the pseudoscalar $B_c([1^1S_0])$ and $\alpha = 0$, $\beta = 1$ for the vector $B_c^*([1^3S_1])$. The radial part of the momentum space wave function $\phi(q)$ is related to the space-time wave function at origin by the integration:

$$i\int\frac{d^4q}{(2\pi)^4}\phi(q) = \psi(0)\,.$$

B. Motivation and basic formulae for decomposing the gluon self-coupling vertices

In Ref.[21], a method is proposed for treating the amplitude of the processes, which contain massless fermions and non-abelian gauge boson(s), in order to make the result compact and to avoid numerical cancellations between very large numbers. The authors of Ref.[21] group the Feynman diagrams of the concerned process into gauge-invariant subsets according to how the lines of the gauge bosons attach to the fermion lines. They then choose convenient gauges for the subsets independently of each other (not a unique gauge for the whole process), and finally they obtain a compact result, when all terms of the amplitude are

written according to the helicities of the fermions. The key point of the approach (helicity technique) is that when all the massless fermions are written on helicity state basis, then it is straightforward to choose convenient gauges for all subsets. If massive fermions are involved in the concerned process and one wishes to use the same technique, then one needs to generalize it. Some rearrangements, such as replacing one massive fermion by two massless fermions *etc*, should be made, and the gauge choice for each subset is more complicated than in the massless cases. In the present case for the subprocess $gg \to B_c + b + \bar{c}$, a unique gauge for the whole amplitude is more practical. Apart from the gauge choice, we apply the techniques of Ref. [21] as much as possible to make the program compact. The polarization vectors of the gluons are replaced by γ-matrix elements of massless fermion helicity states and the color factors are dealt with independently from the Dirac γ-matrix strings. Furthermore, we try to make the amplitude more symmetric by applying a decomposition of the terms when writing the program. This is achieved by decomposing first the terms, which contain three- or/and four-gluon vertices, into terms without self-interactions of gluons. Then, according to the structure of the contained fermion lines, some of the decomposed terms are chosen as 'coordinators', which would be called as the typical ones, so that all the other terms, referring to the Feynman diagrams, may be 'expressed' by the 'typical ones'. Therefore when writing the program, only different 'typical Feynman diagrams' need to be written precisely, while the non-typical ones may be generated by means of the typical ones according to the relationship (expression). In this section, we show how to decompose the terms in the Feynman diagrams containing three- or four-gluon vertex(ices) into terms similar to the typical ones, disregarding the difference in color factors, and list the results for the typical Feynman diagrams.

First of all, let us introduce a massless fermion with an arbitrary light-like reference momentum q ($q^2 = 0$) and its relevant helicity spinors ($|q_\pm\rangle = \frac{1\pm\gamma_5}{2}|q\rangle$ and $\not{q}|q\rangle = 0$), and then construct the requested massive fermion four-spinors $u(p)$ and $v(p)$ with momentum p ($p^2 = m^2$) in terms of $|q_\pm\rangle$ as follows:

$$\begin{aligned} u_s(p) &= \frac{1}{\sqrt{2p\cdot q}}(\not{p} + m)|q_h\rangle\,, \\ v_s(p) &= \frac{1}{\sqrt{2p\cdot q}}(\not{p} - m)|q_{-h}\rangle\,, \end{aligned} \tag{11}$$

where $s = \pm\frac{1}{2}$ is the spin of the massive spinors, while $h = \pm$ is the helicity of the massless spinor. For convenience we adopt the explicit form for the polarization vectors $\epsilon^\pm$ of the gluon

with momentum k as in CALKUL. When the helicity states $|k_\pm\rangle$ and $|q'_\pm\rangle$ of two massless fermions are defined as $|q_\pm\rangle$, but the fermions have a light-like momentum k ($k^2 = 0$) and a referred one q' ($q'^2 = 0$) respectively, the polarization vectors $\epsilon^\pm$ of the gluon with momentum k may be represented as follows:

$$\begin{aligned}
\epsilon^+_\mu(k,q') &= \frac{\langle q'_-|\gamma_\mu|k_-\rangle}{\sqrt{2}\langle q'\cdot k\rangle}\,,\\
\epsilon^-_\mu(k,q') &= \frac{\langle q'_+|\gamma_\mu|k_+\rangle}{\sqrt{2}\langle q'\cdot k\rangle^*}\,,\\
\not{\epsilon}^+(k,q') &= \frac{\sqrt{2}}{\langle q'\cdot k\rangle}(|k_-\rangle\langle q'_-| + |q'_+\rangle\langle k_+|)\,,\\
\not{\epsilon}^-(k,q') &= \frac{\sqrt{2}}{\langle q'\cdot k\rangle^*}(|k_+\rangle\langle q'_+| + |q'_-\rangle\langle k_-|)\,.
\end{aligned} \tag{12}$$

Throughout the paper $\langle q'\cdot k\rangle$ and $\langle q'\cdot k\rangle^*$ denotes $\langle q'_-|k_+\rangle$ and its complex conjugation respectively.

Because the light-like momenta q and q' can be chosen arbitrarily, we choose them to be the same as a light-like momentum q_0, which is the reference momentum for all massive spinors and gluon polarization vectors. We take one gauge for the whole set of 36 Feynman diagrams, that is convenient here and different from CALKUL where different gauges are taken for different gauge-invariant subsets.

The gluon self-coupling vertices do not adapt well for being simplified by using the polarization vector in calculating the amplitude. Hence an effort to replace the part with the gluon self-coupling of the diagrams by the so-called QED-like ones (without gluon self-coupling) is described here. This approach is not straightforward, due to the fact that the gluon self-coupling diagrams with massive quarks can not be mapped completely into the QED-like diagrams as in the case of the massless quark condition[21]. In the massive quark case, some additional functions need to be introduced. Fortunately, for the 'simple' subprocess, these 'extra' functions for the three-gluon vertices are just parts of the diagrams with four-gluon vertices. Thus the diagrams involving four-gluon coupling vertices just need to be decomposed according to their color factors and there is no need to reduce their γ matrix and spinor factors any further.

To decompose Feynman diagrams with self-interactions into those without any, we need to deal with some of the so-called 'basic structures'. The number of the 'basic structures' required for a specific process increases with the number of the gluons involved in the

concerned process. For the subprocess, $gg \to B_c(B_c^*) + b + \bar{c}$, to convert the necessary parts to the 'basic structures', only the parts containing a three-gluon coupling vertex have to be decomposed. Thus let us outline the decomposition for the concerned subprocess.

The decomposition of a three-gluon coupling vertex is shown in Fig.6 (the first structure): a three-gluon vertex $f^{abc}T_{\mu\nu\delta}(k_1, K, k_2)$ through a gluon propagator $-ig_{vv'}/K^2$ couples to a quark line with a quark-gluon-quark vertex $T_b\gamma_{\nu'}$, where $K = -(k_1 + k_2) = -(Q + Q')$, and f^{abc}, T_b are color factors at the two vertices. It is

$$M^{ac}_{\mu\delta}(k_1, k_2, Q, Q') = -g_s^2 f^{abc} T_b T_{\mu\nu\delta}(k_1, K, k_2) \frac{-ig_s g^{vv'}}{K^2} \gamma_{\nu'} \,, \tag{13}$$

where Q and Q' are the momenta of the fermion legs at the vertex. Since

$$T_{\mu\nu\delta}(k_1, K, k_2) = (k_1 - K)_\delta g_{\mu\nu} + (K - k_2)_\mu g_{\nu\delta} + (k_2 - k_1)_\nu g_{\mu\delta} \,, \tag{14}$$

so the precise expression is

$$\begin{aligned} M^{ac}_{\mu\delta}(k_1, k_2, Q, Q') \;=\; & g_s^2 f^{abc} T_b \frac{i}{K^2} \Big((k_1 + Q + Q')_\delta \gamma_\mu + k_{1\mu}\gamma_\delta - \not{Q}'\gamma_\mu\gamma_\delta - \gamma_\mu \not{Q}'\gamma_\delta \\ & - \gamma_\delta \not{Q}\gamma_\mu - \gamma_\delta\gamma_\mu \not{Q} + (\not{Q} + \not{Q}' - 2\not{k}_1) g_{\mu\delta} \Big) \\ =\; & g_s^2 f^{abc} T_b \frac{i}{K^2} \Big(\gamma_\delta(\not{k}_1 - \not{Q} + m)\gamma_\mu - \gamma_\mu(\not{k}_2 - \not{Q} + m)\gamma_\delta + \\ & (\not{Q}' - m)(\gamma_\delta\gamma_\mu - g_{\mu\delta}) + \\ & (\gamma_\mu\gamma_\delta - g_{\mu\delta})(\not{Q} + m) + k_{2\delta}\gamma_\mu - k_{1\mu}\gamma_\delta \Big) \,. \end{aligned} \tag{15}$$

If the factor g_s^2, the propagator scalar factor and the color factor are disregarded, and the symbol $\simeq$ is used for an equality modulo these factors, we have

$$\begin{aligned} M^{ac}_{\mu\delta} \;\simeq\; & \gamma_\delta(\not{k}_1 - \not{Q} + m)\gamma_\mu - \gamma_\mu(\not{k}_2 - \not{Q} + m)\gamma_\delta + (\not{Q}' - m)(\gamma_\delta\gamma_\mu - g_{\mu\delta}) \\ & + (\gamma_\mu\gamma_\delta - g_{\mu\delta})(\not{Q} + m) + k_{2\delta}\gamma_\mu - k_{1\mu}\gamma_\delta + \cdots \,, \end{aligned} \tag{16}$$

where m is the mass of the fermion. Here the gluons and fermions may not be on-shell. If the first and the second terms on the right-hand side are embedded in the diagrams, the basic QED-like diagrams may be obtained, while the rest terms $\cdots$ on the right-hand side can be absorbed into several extra functions.

To relate to the 'basic structures', two further decompositions are shown in Fig.7 (the second structure) and Fig.8 (the third structure) respectively: a three-gluon vertex

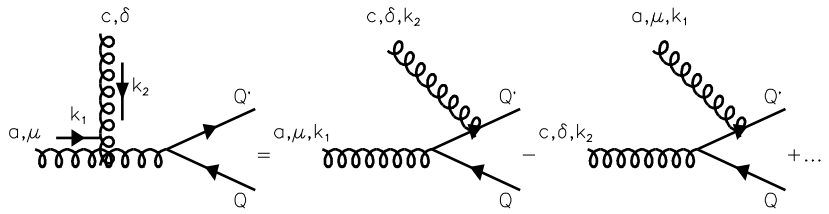

FIG. 6: The three-gluon coupling vertex is decomposed as in Eq.(16): the first two terms are the 'basic QED-like' terms and the 'remaining' terms are expressed by several extra basic functions.

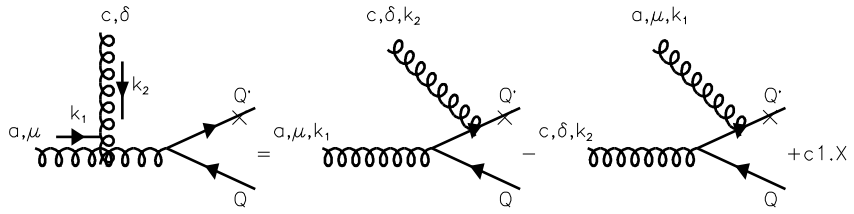

FIG. 7: Reduction of the basic structure with a three gluon vertex: the first two terms correspond to the basic QED-like diagrams and the symbol '×' means a quark gluon vertex $T_d\gamma_\alpha$.

$f_{abc}T_{\mu\nu\delta}(k_1, k_1+k_2, k_2)$ is coupled to a quark line, which has two vertices of quark-gluon-quark $T_b\gamma_\nu$ and $T_d\gamma_\alpha$. To be precise, we label the latter vertex with the symbol '×' on the quark line. In the present case the two external quark lines are both on-shell and then these two structures can be simplified by using the on-shell conditions

$$\bar{u}(Q')(\not{Q}' - m) = 0\,, \quad (\not{Q} + m)v(Q) = 0\,. \tag{17}$$

The contribution from the corresponding part in Fig.7 is:

$$M^{acd}_{\mu\delta\alpha}(k_1,k_2,Q,Q') \;=\; -g_s f^{abc}T_bT_d\bar{u}(Q')\gamma_\alpha\frac{i(\not k_1+\not k_2-\not Q+m)}{(k_1+k_2-Q)^2-m^2}\cdot \\ T_{\mu\nu\delta}(k_1,K,k_2)\frac{-ig_s g^{vv'}}{K^2}\gamma_{\nu'}v(Q)\,. \qquad (18)$$

With Eq.(16) and the on-shell condition Eq.(17) for the two external fermion legs, we obtain

$$\begin{aligned} M^{acd}_{\mu\delta\alpha}(k_1,k_2,Q,Q') \;\simeq\; & \bar{u}(Q')\gamma_\alpha(\not k_1+\not k_2-\not Q+m)\Big(\gamma_\delta(\not k_1-\not Q+m)\gamma_\mu-\gamma_\mu(\not k_2-\not Q+m)\gamma_\delta\Big)v(Q) \\ & +\Big(m_1^2+m_2^2+2k_1\cdot k_2-2Q\cdot k_1-2Q\cdot k_2\Big)\bar{u}(Q')\gamma_\alpha(\gamma_\delta\gamma_\mu-g_{\mu\delta})v(Q)+ \\ & \bar{u}(Q')\gamma_\alpha\Big(k_{2\delta}(\not k_1+\not k_2)\gamma_\mu-k_{1\mu}(\not k_1+\not k_2)\gamma_\delta-2k_{2\delta}Q_\mu+2k_{1\mu}Q_\delta\Big)v(Q) \\ =\; & \bar{u}(Q')\gamma_\alpha(\not k_1+\not k_2-\not Q+m)\Big(\gamma_\delta(\not k_1-\not Q+m)\gamma_\mu-\gamma_\mu(\not k_2-\not Q+m)\gamma_\delta\Big)v(Q) \\ & +(c1\cdot X)+\cdots\,, \end{aligned} \qquad (19)$$

where '$\simeq$' means that the factor g_s^2, the propagator scalar factor and the color factor have been omitted. The first term is for the basic QED-like diagrams. The second term $(c1\cdot X)$ where

$$c1 = m_1^2+m_2^2+2k_1\cdot k_2-2Q\cdot k_1-2Q\cdot k_2$$

and

$$X = \bar{u}(Q')\gamma_\alpha\{\gamma_\delta\gamma_\mu-g_{\mu\delta}\}v(Q)$$

will be treated below. The third term '$\cdots$', in fact, does not contribute to the amplitude, no matter whether the gluons are virtual or real. The proof is that when both the concerned gluons are real, it is easy to show that the remaining terms give zero contribution by using the relation $\epsilon(k_l)\cdot k_l = 0$ $(l=1,2)$. When one of the concerned gluons is virtual, the gluon with momentum k_2 for example, $k_{2\delta}$ will always couple to a 'simple' quark line as $\bar{u}(R)\gamma_\delta v(R')$ at the lowest order for the amplitude of the considered process $gg\to B_c(B_c^*)+\bar{c}+b$, where u and v are the quark and anti-quark spinors, and $k_2 = R+R'$ (the momenta R, R' satisfy the on-shell condition: $R^2 = R'^2 = m^2$, where m is the mass of the quark). It is easy to show that the contribution of the remaining terms is zero by using a similar on-shell condition as Eq.(17). Therefore, in Fig.7 and in the following Fig.8, the remaining terms have not been shown explicitly.

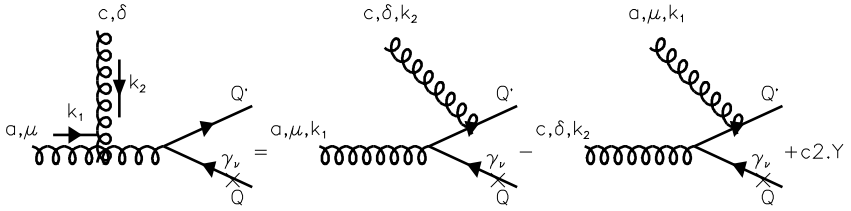

FIG. 8: Dividing the basic topology including the three gluon vertex, where the first two terms correspond to the 'basic QED-like' diagrams and the symbol '$\times$' means a quark gluon vertex $T_d\gamma_\alpha$.

In the same way as above, the contribution from the corresponding part in Fig.8 is:

$$
\begin{aligned}
M^{acd}_{\mu\delta\alpha}(k_1,k_2,Q,Q') \;\simeq\; & \bar{u}(Q')\Big(\gamma_\delta(\not{Q}'-\not{k}_2+M)\gamma_\mu-\gamma_\mu(\not{Q}'-\not{k}_1+M)\gamma_\delta\Big)(\not{Q}'-\not{k}_1-\not{k}_2+M)\cdot \\
& \gamma_\alpha v(Q)+\Big(m_1^2+m_2^2+2k_1\cdot k_2-2Q'\cdot k_1-2Q'\cdot k_2\Big)\bar{u}(Q')(\gamma_\delta\gamma_\mu-g_{\mu\delta})\cdot \\
& \gamma_\alpha v(Q)+\bar{u}(Q')\Big(-k_{2\delta}\gamma_\mu(\not{k}_1+\not{k}_2)+k_{1\mu}\gamma_\delta(\not{k}_1+\not{k}_2)+2k_{2\delta}Q'_\mu+ \\
& 2k_{1\mu}Q'_\delta\Big)\gamma_\alpha v(Q)+(c2\cdot Y)+\cdots\,, \qquad (20)
\end{aligned}
$$

where again the factor g_s^2, the scalar factor of the propagators and the color factor have been omitted. The first two terms correspond to the basic QED-like diagrams, and the term which is expressed by $(c2\cdot Y)$ is defined as

$$c2=m_1^2+m_2^2+2k_1\cdot k_2-2Q'\cdot k_1-2Q'\cdot k_2\,,$$

where Y is a new extra function

$$Y=\bar{u}(Q')\{\gamma_\delta\gamma_\mu-g_{\mu\delta}\}\gamma_\alpha v(Q).$$

Similarly as for the second structure in Eq.(19), the remaining terms in the present structure contribute nothing, thus in Fig.8, they have not been shown explicitly.

Having made all the preparations above, and performing all the possible interchanges, such as gluon exchange, quark and anti-quark exchange, we relate each of the terms in the diagrams to a combination of those with the basic QED-like diagrams ('coordinators'), including the introduced two 'extra' functions as well.

C. The decomposition

The B_c meson is a double-heavy weak-binding state. According to pQCD each term of the amplitude for the subprocess may be factorized into two factors: that of perturbative $gg \to b + \bar{b} + c + \bar{c}$ (all the quarks are on shell) and that of non-perturbative $c + \bar{b} \to B_c$. The binding wave function in the Bethe-Salpeter framework may be used to dictate the non-perturbative one, and approximately written as Eq.(10). To carry out the factorization of the amplitude, one may apply Eq.(10) and the two equations:

$$\begin{aligned} \not{q}_{c1} + m_c &= \sum_s u(q_{c1}, s)\bar{u}(q_{c1}, s) \simeq \alpha_1(\not{P} + M)\,, \\ \not{q}_{b2} - m_b &= \sum_s v(q_{b2}, s)\bar{v}(q_{b2}, s) \simeq -\alpha_2(\not{P} + M) \end{aligned} \tag{21}$$

to each term in the amplitude in Eqs.(4-8) with the corresponding factors $\bar{\chi}_P(q)$.

Then the general structure of the amplitude in 'explicit helicity' form turns to

$$\begin{aligned} M_i^{(\lambda_1,\lambda_4,\lambda_5,\lambda_6)}(q_{b1}, q_{b2}, q_{c1}, q_{c2}, k_1, k_2) &= \sum_{\lambda_2,\lambda_3} C_i X_i D_1 B_{Fi}^{(\lambda_1,\lambda_2,\lambda_3,\lambda_4,\lambda_5,\lambda_6)}(q_{b1}, q_{b2}, q_{c1}, q_{c2}, k_1, k_2) \cdot \\ & \quad D_2 B_{B_c(B_c^*)}^{(\lambda_2,\lambda_3)}(q_{b2}, q_{c1}), \end{aligned} \tag{22}$$

where $i = 1, \cdots, 36$ (or labelled as Feynman diagrams: $1a, 1b, \cdots, 5d$, respectively), λ_j ($j = 1, \cdots, 6$) denote the helicities (spins) of the quarks and gluons respectively appearing in the two factorized 'processes' $gg \to b + \bar{b} + c + \bar{c}$ and $c + \bar{b} \to B_c$. Note that from now on, we change the notation of the helicities of the particles in the processes as: λ_1 denotes the helicity of b, λ_2 that of $\bar{b}$, λ_3 that of c, λ_4 that of $\bar{c}$; whereas λ_5, instead of λ_1 in Eqs.(4-8), denotes that of gluon-1 and λ_6, instead of λ_2 in Eqs.(4-8), denotes that of gluon-2. Here C_i, X_i denote the color factor and the scalar factor from all the propagators as a whole for the ith-diagram, respectively. $B_{Fi}^{(\lambda_1,\lambda_2,\lambda_3,\lambda_4,\lambda_5,\lambda_6)}(q_{b1}, q_{b2}, q_{c1}, q_{c2}, k_1, k_2)$ and $B_{B_c(B_c^*)}^{(\lambda_2,\lambda_3)}(q_{b2}, q_{c1})$ are the amplitudes corresponding to the 'free quark part' $g(k_1, \lambda_5)g(k_2, \lambda_6) \to b(q_{b1}, \lambda_1) + \bar{b}(q_{b2}, \lambda_2) + c(q_{c1}, \lambda_3) + \bar{c}(q_{c2}, \lambda_4)$ (all the quarks are on-shell) and the 'bound state part' $c(q_{c1}, \lambda_3) + \bar{b}(q_{b2}, \lambda_2) \to B_c(B_c^*)$, respectively. Substituting Eq.(11), we have

$$\begin{aligned} B_{Fi}^{(\lambda_1,\lambda_2,\lambda_3,\lambda_4,\lambda_5,\lambda_6)}(q_{b1}, q_{b2}, q_{c1}, q_{c2}, k_1, k_2) &= \langle q_{0\lambda_1}|(\not{q}_{b1} + m_b)\Gamma_{1i}(\not{q}_{b2} - m_b)|q_{0\lambda_2}\rangle \cdot \\ & \quad \langle q_{0\lambda_3}|(\not{q}_{c1} + m_c)\Gamma_{2i}(\not{q}_{c2} - m_c)|q_{0\lambda_4}\rangle\,, \end{aligned} \tag{23}$$

$$\begin{aligned} B_{B_c(B_c^*)}^{(\lambda_2,\lambda_3)}(q_{b2}, q_{c1}) = \langle q_{0\lambda_2}|(\alpha\gamma_5 \;+\; & \beta\not{\epsilon}(s_z))\frac{(\not{P} + M)}{2\sqrt{M}}\psi(0)|q_{0\lambda_3}\rangle\,, \\ (\alpha = 1,\;\; \beta = 0\,,\;\; for\;\; B_c[1^1S_0]; \qquad & \alpha = 0,\;\; \beta = 1\,,\;\; for\;\; B_c^*[1^3S_1]) \end{aligned} \tag{24}$$

where $|q_0\lambda_r\rangle$ and $\langle q_0\lambda_r|$ ($\lambda_r = \pm,\ r = 1,\cdots,4$) are the introduced helicity states of the massless fermion q_0 which specifically relate to those of massive fermions with the momentum p and mass m as in Eq.(11), $\Gamma_{1i,2i}$ are the explicit strings of Dirac γ matrices corresponding to i-th Feynman diagram which contain the gluon helicities λ_5 and λ_6. $D_1 = \frac{1}{\sqrt{2q_{b1}\cdot q_0}}\frac{1}{\sqrt{2q_{b2}\cdot q_0}}\frac{1}{\sqrt{2q_{c1}\cdot q_0}}\frac{1}{\sqrt{2q_{c2}\cdot q_0}}$ and $D_2 = \frac{1}{\sqrt{2q_{c1}\cdot q_0}}\frac{1}{\sqrt{2q_{b2}\cdot q_0}}$ are the two common normalization factors.

The function $D_2 B^{(\lambda_2,\lambda_3)}_{B_c(B_c^*)}(q_{b2}, q_{c1})$, which contains the bound state wave function, is:

$$D_2 B^{(\lambda_2,\lambda_3)}_{B_c}(q_{b2}, q_{c1}) = \frac{\psi(0)\sqrt{M}}{2\sqrt{m_b m_c}}\delta_{\lambda_2,\lambda_3}(\delta_{\lambda_2-} - \delta_{\lambda_2+}) \tag{25}$$

for $B_c[^1S_1]$, and

$$\begin{aligned} D_2 B^{(\lambda_2,\lambda_3)}_{B_c^*}(q_{b2}, q_{c1}) \ =\ & \frac{\psi(0)\sqrt{M}}{2\sqrt{m_b m_c}}\delta_{\lambda_2,\lambda_3}(\delta_{\lambda_2+} + \delta_{\lambda_2-})\left(\frac{M\epsilon(s_z)\cdot q_0}{P\cdot q_0}\right) + \frac{\psi(0)\sqrt{M}}{2\sqrt{m_b m_c}}\left(\frac{1}{2P\cdot q_0}\right)\cdot \\ & \langle q_{0\lambda_2}|\not{\epsilon}(s_z)\not{P}|q_{0\lambda_3}\rangle \end{aligned} \tag{26}$$

for $B_c^*[^3S_1]$.

These 36 functions, $B^{(\lambda_1,\lambda_2,\lambda_3,\lambda_4,\lambda_5,\lambda_6)}_{Fi}(q_{b1}, q_{b2}, q_{c1}, q_{c2}, k_1, k_2)$, can be constructed by nine 'basic ones' which correspond to Fig.3a, Fig.3b, Fig.3c, Fig.3d, Fig.5d (two basic functions), Fig.1a, Fig.1c and Fig.1e, and by performing all the possible interchanges of the initial gluons and the two quark lines. In fact, the functions which correspond to Fig.3c and Fig.3d can be obtained from those in Fig.3a and Fig.3b by interchanging the initial gluons and the quark lines in the diagrams, and in the following section we will show that the functions corresponding to Fig.1a and Fig.1c can also be expressed by other seven 'basic functions', although here we still treat those four functions as 'basic ones', in order to treat them on an equal footing.

We use $E_{m,j,k}(q_{b1}, q_{b2}, q_{c1}, q_{c2}, k_1, k_2)\,,\ (m = 1,2,\cdots,9;\ j = 1,\cdots,4;\ k = 1,2,\cdots 64)$ to denote the 'basic functions', where k denotes 64 possible helicities (spins) corresponding to possible 'values' of $(\lambda_1,\lambda_2,\lambda_3,\lambda_4,\lambda_5,\lambda_6)$ as shown in Table I, and the correspondences of the functions to the Feynman diagrams are shown in Table II and Table III. Here j means the four possible interchanges: 1 means identical (without any interchange), 2 means interchange of the gluons, 3 means interchange of the quark and the anti-quark, and 4 means interchange of the gluons and the quark and anti-quark. When applying the interchange among the particles, the symmetries of the decomposed amplitude guarantee that every

TABLE I: The correspondence between $k = 1, \cdots, 64$ and $\lambda_1 = \pm, \lambda_2 = \pm, \lambda_3 = \pm, \lambda_4 = \pm, \lambda_5 = \pm, \lambda_6 = \pm$, which stand for the helicities of the particles in the process.

k	λ_1	λ_2	λ_3	λ_4	λ_5	λ_6	k	λ_1	λ_2	λ_3	λ_4	λ_5	λ_6	k	λ_1	λ_2	λ_3	λ_4	λ_5	λ_6	k	λ_1	λ_2	λ_3	λ_4	λ_5	λ_6
1	+	+	+	+	+	+	17	−	−	−	−	−	−	33	+	+	−	+	+	+	49	−	−	+	−	−	−
2	+	+	+	+	+	−	18	−	−	−	−	−	+	34	+	+	−	+	+	−	50	−	−	+	−	−	+
3	+	+	+	+	−	+	19	−	−	−	−	+	−	35	+	+	−	+	−	+	51	−	−	+	−	+	−
4	+	+	+	+	−	−	20	−	−	−	−	+	+	36	+	+	−	+	−	−	52	−	−	+	−	+	+
5	+	+	+	−	+	+	21	−	−	−	+	−	−	37	+	+	−	−	+	+	53	−	−	+	+	−	−
6	+	+	+	−	+	−	22	−	−	−	+	−	+	38	+	+	−	−	+	−	54	−	−	+	+	−	+
7	+	+	+	−	−	+	23	−	−	−	+	+	−	39	+	+	−	−	−	+	55	−	−	+	+	+	−
8	+	+	+	−	−	−	24	−	−	−	+	+	+	40	+	+	−	−	−	−	56	−	−	+	+	+	+
9	+	−	−	+	+	+	25	−	+	+	−	−	−	41	+	−	+	+	+	+	57	−	+	−	−	−	−
10	+	−	−	+	+	−	26	−	+	+	−	−	+	42	+	−	+	+	+	−	58	−	+	−	−	−	+
11	+	−	−	+	−	+	27	−	+	+	−	+	−	43	+	−	+	+	−	+	59	−	+	−	−	+	−
12	+	−	−	+	−	−	28	−	+	+	−	+	+	44	+	−	+	+	−	−	60	−	+	−	−	+	+
13	+	−	−	−	+	+	29	−	+	+	+	−	−	45	+	−	+	−	+	+	61	−	+	−	+	−	−
14	+	−	−	−	+	−	30	−	+	+	+	−	+	46	+	−	+	−	+	−	62	−	+	−	+	−	+
15	+	−	−	−	−	+	31	−	+	+	+	+	−	47	+	−	+	−	−	+	63	−	+	−	+	+	−
16	+	−	−	−	−	−	32	−	+	+	+	+	+	48	+	−	+	−	−	−	64	−	+	−	+	+	+

term may be expressed by the basic functions with helicities and momenta of the particles in the process. For all the functions $E_{m,j,k}$, with m, j being fixed, they are related to each other by proper complex conjugation with or without changing the whole sign. To write the program, and to apply these relations of the element functions among different helicity states conveniently, we take the correspondence between k and $(\lambda_1, \lambda_2, \lambda_3, \lambda_4, \lambda_5, \lambda_6)$ as described in Table I. Thus we have now

$$\begin{aligned} B_{Fi}^{(\lambda_1,\lambda_2,\lambda_3,\lambda_4,\lambda_5,\lambda_6)}(q_{b1}, q_{b2}, q_{c1}, q_{c2}, k_1, k_2) &\equiv B_{Fi}^{(k)}(q_{b1}, q_{b2}, q_{c1}, q_{c2}, k_1, k_2) \\ &= \sum_{m=1}^{9} \sum_{j=1}^{4} f_{i,m,j} E_{m,j,k} \,. \end{aligned} \tag{27}$$

Here i and k denote the 36 Feynman diagrams (terms) and the 64 possible helicities of all the

TABLE II: The expansion coefficients $f_{i,m,j}$ for the functions $B^{(k)}_{Fi}(q_{b1}, q_{b2}, q_{c1}, q_{c2}, k_1, k_2)$ which are grouped into the cb subset directly or indirectly through a proper decomposition (the coefficients $f_{i,m,j}$ are not listed here if they are equal to zero in a whole row).

	$j=1$				
m	1	2	3	4	5
$f_{3a,m,j}$	1	0	0	0	0
$f_{3b,m,j}$	0	1	0	0	0
$f_{3d,m,j}$	0	0	1	0	0
$f_{3e,m,j}$	0	0	0	1	0
$f_{4c,m,j}$	-1	0	1	0	$-2(q_{c2}\cdot k_1)$
$f_{4d,m,j}$	0	-1	0	1	$2(q_{c1}\cdot k_1)$
$f_{4f,m,j}$	1	-1	0	0	$2(q_{b1}\cdot k_2)$
$f_{4g,m,j}$	0	0	1	-1	$-2(q_{b2}\cdot k_2)$
$f_{5b,m,j}$	1	-1	-1	1	$s_b + s_c - s_2$

particles in the two factorized processes. The correspondence of helicities on $k = 1, \cdots, 64$ is given as described in Table I. The 36 functions $i = 1, \cdots, 36$ are labelled as the 36 Feynman diagrams, *i.e.* $i = 1a, 1b, \cdots, 5d$. The coefficient $f_{i,m,j}$ corresponding to QED-like diagrams can be directly read out easily, but as for the diagrams involving three- and four- gluon vertices we decompose them by applying the formulae obtained in the subsection B.

D. The amplitude $B^{(k)}_{Fi}(q_{b1}, q_{b2}, q_{c1}, q_{c2}, k_1, k_2)$

All the terms for the subprocess may be divided into four subsets according to the manner how the gluons attach to the fermion lines. For the cc set, both gluons attach directly to the c-quark line; for the cb set, the gluon-1 attaches to the c-quark line while the gluon-2 attaches to the b-quark line; for the bc set, the gluon-1 attaches to the b-quark line while the gluon-2 attaches to the c-quark line; for the bb set, both gluons attach directly to the b-quark line in the relevant Feynman diagrams. The diagrams involving three- and four-gluon vertex (vertices) which are shown in Fig.4 and Fig.5 are decomposed by applying

the decomposition formulae in subsection B. Hence each of the terms corresponding to the diagrams in general turns to four terms and then they may be put into four subsets separately according to the resulting characteristics of the decomposed term. The results are shown in Table II and Table III. In Table II and Table III, we list the exact results for the *cb* and *cc* sets, and the results for the *bc* and *bb* sets by performing interchanges of the initial gluons and the final quark lines. In Table II and Table III one may see, for example, how the Feynman diagrams in Figs.4c, 4d and Fig.5b are decomposed, and how each of the decomposed term is divided into a *cb* or a *cc* set. We summarize the relations among the functions $B_{Fi}^{(k)}(q_{b1}, q_{b2}, q_{c1}, q_{c2}, k_1, k_2)$ and show them in Table II and Table III respectively. In Table II, the functions $B_{Fi}^{(k)}(q_{b1}, q_{b2}, q_{c1}, q_{c2}, k_1, k_2)$ are listed either directly or through a proper decomposition in order to relate them to the *cb* subset through functions $E_{m,j,k}$ and suitable coefficients $f_{i,m,j}$. In Table III, the functions $B_{Fi}^{(k)}(q_{b1}, q_{b2}, q_{c1}, q_{c2}, k_1, k_2)$ are listed either directly or indirectly through a proper decomposition relating to the *cc* subset via suitable coefficients $f_{i,m,j}$. In addition, in Table III, we have decomposed the matrix element M_{5d} of Fig.5d, as shown in Eq.(8), into three parts according to the three different color factors: $C_{5d1} = C_{2ij} + C_{3ij} - C_{1ij} - C_{4ij}$, $C_{5d2} = C_{5ij} - C_{1ij} + C_{3ij}$, $C_{5d3} = C_{5ij} - C_{2ij} + C_{4ij}$. The parameters used in Table II and Table III are as follows: $s_b = (q_{b1} + q_{b2})^2$, $s_c = (q_{c1} + q_{c2})^2$, $s_2 = (k_2 - q_{b1} - q_{b2})^2$, $f_1 = 2(q_{c1} - q_{c2}) \cdot k_2 + s_b$, $f_2 = 2(q_{c1} - q_{c2}) \cdot k_1 + s_b$, $f_3 = 2k_1 \cdot k_2 - 2q_{c2} \cdot k_1 - 2q_{c2} \cdot k_2$, $f_4 = 2k_1 \cdot k_2 - 2q_{c1} \cdot k_1 - 2q_{c1} \cdot k_2$.

E. The 'basic functions' $E_{m,j,k}(q_{b1}, q_{b2}, q_{c1}, q_{c2}, k_1, k_2)$

To obtain the nine 'basic functions' $E_{m,j,k}$ $(m = 1, \cdots, 9)$, let us first define the functions which correspond to various kinds of quark lines (different γ structures of the fermion lines), where $q_1^2 = q_2^2 = m^2$ and $q_0^2 = k^2 = k_1^2 = k_2^2 = 0$:

$$
\begin{aligned}
f_0(q_1, q_2, \lambda_1, \lambda_2) &= \langle q_{0\lambda_1} | (\not{q}_1 + m)\gamma_\delta(\not{q}_2 - m) | q_{0\lambda_2} \rangle \,, \\
f_1(q_1, q_2, k, \lambda_1, \lambda_2, \lambda_3) &= \langle q_{0\lambda_1} | (\not{q}_1 + m)\gamma_\delta(\not{k} - \not{q}_2 + m)\not{\epsilon}^{\lambda_3}(k, q_0)(\not{q}_2 - m) | q_{0\lambda_2} \rangle \,, \\
f_2(q_1, q_2, k, \lambda_1, \lambda_2, \lambda_3) &= \langle q_{0\lambda_1} | (\not{q}_1 + m)\not{\epsilon}^{\lambda_3}(k, q_0)(\not{q}_1 - \not{k} + m)\gamma_\delta(\not{q}_2 - m) | q_{0\lambda_2} \rangle \,, \\
f_3(q_1, q_2, k, \lambda_1, \lambda_2, \lambda_3) &= \langle q_{0\lambda_1} | (\not{q}_1 + m)\not{\epsilon}^{\lambda_3}(k, q_0)(\not{q}_2 - m) | q_{0\lambda_2} \rangle \,, \\
f_4(q_1, q_2, k_1, k_2, \lambda_1, \lambda_2, \lambda_3, \lambda_4) &= \langle q_{0\lambda_1} | (\not{q}_1 + m)\gamma_\delta(\not{k}_1 + \not{k}_2 - \not{q}_2 + m)\not{\epsilon}^{\lambda_3}(k_1, q_0) \cdot \\
&\quad (\not{k}_2 - \not{q}_2 + m)\not{\epsilon}^{\lambda_4}(k_2, q_0)(\not{q}_2 - m) | q_{0\lambda_2} \rangle \,,
\end{aligned}
$$

TABLE III: The expansion coefficients $f_{i,m,j}$ for the functions $B^{(k)}_{Fi}(q_{b1}, q_{b2}, q_{c1}, q_{c2}, k_1, k_2)$ which are grouped into the cc subset directly or indirectly through a proper decomposition (the coefficients $f_{i,m,j}$, which are equal to zero in a whole row, are not listed here).

	$j=1$					$j=2$				
m	6	7	8	9	5	6	7	8	9	5
$f_{1a,m,j}$	1	0	0	0	0	0	0	0	0	0
$f_{1b,m,j}$	0	0	0	0	0	1	0	0	0	0
$f_{1c,m,j}$	0	1	0	0	0	0	0	0	0	0
$f_{1d,m,j}$	0	0	0	0	0	0	1	0	0	0
$f_{1e,m,j}$	0	0	1	0	0	0	0	0	0	0
$f_{1f,m,j}$	0	0	0	0	0	0	0	1	0	0
$f_{1g,m,j}$	1	0	0	$\frac{f_3}{2}$	0	-1	0	0	$-\frac{f_3}{2}$	0
$f_{1h,m,j}$	0	0	1	$\frac{f_4}{2}$	$2f_4$	0	0	-1	$\frac{f_4}{2}$	$-2f_4$
$f_{4a,m,j}$	-1	1	0	$2q_{c2}\cdot k_2$	0	0	0	0	0	$-2q_{c2}\cdot k_2$
$f_{4b,m,j}$	0	0	0	0	$4q_{c1}\cdot k_2$	0	-1	1	$-2q_{c1}\cdot k_2$	$-2q_{c1}\cdot k_2$
$f_{4c,m,j}$	0	0	0	0	$-2q_{c2}\cdot k_1$	-1	1	0	$2q_{c2}\cdot k_1$	0
$f_{4d,m,j}$	0	-1	1	$-2q_{c1}\cdot k_1$	$-2q_{c1}\cdot k_1$	0	0	0	0	$4q_{c1}\cdot k_2$
$f_{5a,m,j}$	1	-1	0	$2q_{c2}\cdot k_2$	$-4q_{c1}\cdot k_2$	0	-1	1	$2q_{c1}\cdot k_2$	f_1
$f_{5b,m,j}$	0	-1	1	$2q_{c1}\cdot k_1$	f_2	1	-1	0	$2q_{c2}\cdot k_1$	$-4q_{c1}\cdot k_1$
$f_{5c,m,j}$	-1	0	1	$-\frac{f_3-f_4}{2}$	$2f_4$	1	0	-1	$\frac{f_3-f_4}{2}$	$-2f_4$
$f_{5d1,m,j}$	0	0	0	0	1	0	0	0	0	-1
$f_{5d2,m,j}$	0	0	0	$\frac{1}{2}$	0	0	0	0	$\frac{1}{2}$	-1
$f_{5d3,m,j}$	0	0	0	$\frac{1}{2}$	-1	0	0	0	$\frac{1}{2}$	0

$$
\begin{aligned}
f_5(q_1,q_2,k_1,k_2,\lambda_1,\lambda_2,\lambda_3,\lambda_4) &= \langle q_{0\lambda_1}|(\not{q}_1+m)\not{\epsilon}^{\lambda_3}(k_1,q_0)(\not{q}_1-\not{k}_1+m)\gamma_\delta\cdot \\
&\quad (\not{k}_2-\not{q}_2+m)\not{\epsilon}^{\lambda_4}(k_2,q_0)(\not{q}_2-m)|q_{0\lambda_2}\rangle\,, \\
f_6(q_1,q_2,k_1,k_2,\lambda_1,\lambda_2,\lambda_3,\lambda_4) &= \langle q_{0\lambda_1}|(\not{q}_1+m)\not{\epsilon}^{\lambda_3}(k_1,q_0)(\not{q}_1-\not{k}_1+m)\cdot \\
&\quad \not{\epsilon}^{\lambda_4}(k_2,q_0)(\not{q}_1-\not{k}_1-\not{k}_2+m)\gamma_\delta(\not{q}_2-m)|q_{0\lambda_2}\rangle\,, \\
f_7(q_1,q_2,k_1,k_2,\lambda_1,\lambda_2,\lambda_3,\lambda_4) &= \langle q_{0\lambda_1}|(\not{q}_1+m)\gamma_\delta\not{\epsilon}^{\lambda_3}(k_1,q_0)\not{\epsilon}^{\lambda_4}(k_2,q_0)(\not{q}_2-m)|q_{0\lambda_2}\rangle\,,
\end{aligned}
$$

$$
\begin{aligned}
f_8(q_1,q_2,k_1,k_2,\lambda_1,\lambda_2,\lambda_3,\lambda_4) &= \langle q_{0\lambda_1}|(\not{q}_1+m)\not{\epsilon}^{\lambda_3}(k_1,q_0)\not{\epsilon}^{\lambda_4}(k_2,q_0)\gamma_\delta(\not{q}_2-m)|q_{0\lambda_2}\rangle\,, \\
f_9(q_1,q_2,k_1,k_2,\lambda_1,\lambda_2,\lambda_3,\lambda_4) &= \langle q_{0\lambda_1}|(\not{q}_1+m)\not{\epsilon}^{\lambda_3}(k_1,q_0)\gamma_\delta\not{\epsilon}^{\lambda_4}(k_2,q_0)(\not{q}_2-m)|q_{0\lambda_2}\rangle\,. \quad (28)
\end{aligned}
$$

There are several ways to deal with these fermion lines. In Ref. [24], a systematic way for doing the massive case is proposed. Here we take another and more 'direct' approach. When the massive fermions have time-like momenta q_i $(i=1,2)$ and $\not{q}_i$ are directly connected to $|q_{0\lambda_i}\rangle$ or $\langle q_{0\lambda_i}|$ as in Eq.(28), we may introduce the light-like momenta by defining

$$
q_i' = q_i - \frac{q_i^2}{2q_i\cdot q_0}q_0\,. \quad (29)
$$

Then $\not{q}_i$ for massive fermions can be replaced by the massless ones, $\not{q}'_i$, without any consequences. This is due to the relations

$$
\not{q}_0|q_{0\lambda_i}\rangle = 0 \quad (30)
$$

or

$$
\langle q_{0\lambda_i}|\not{q}_0 = 0\,. \quad (31)
$$

If the massive fermions with momenta q_i $(i=1,2)$ are not directly connected to $|q_{0\lambda_i}\rangle$ or $\langle q_{0\lambda_i}|$, but to another light-like spinor, say $|q'_{0\lambda_i}\rangle$ or $\langle q'_{0\lambda_i}|$, then we may do the same thing if the momentum q_0 and the spinor $|q_{0\lambda_i}\rangle$ or $\langle q_{0\lambda_i}|$ are replaced by q_0' and $|q'_{0\lambda_i}\rangle$ or $\langle q'_{0\lambda_i}|$, accordingly. In this way we can turn the massive terms into massless terms, and then they can be dealt with similarly as in the massless cases[19, 20, 21, 22, 23].

The nine basic functions may be expressed in terms of the above ten functions as

$$
\begin{aligned}
E_{1,1,k} &= f_1(q_{c1},q_{c2},k_1,\lambda_3,\lambda_4,\lambda_5)\cdot f_2(q_{b1},q_{b2},k_2,\lambda_1,\lambda_2,\lambda_6)\,, \\
E_{2,1,k} &= f_2(q_{c1},q_{c2},k_1,\lambda_3,\lambda_4,\lambda_5)\cdot f_2(q_{b1},q_{b2},k_2,\lambda_1,\lambda_2,\lambda_6)\,, \\
E_{3,1,k} &= f_1(q_{c1},q_{c2},k_1,\lambda_3,\lambda_4,\lambda_5)\cdot f_1(q_{b1},q_{b2},k_2,\lambda_1,\lambda_2,\lambda_6)\,, \\
E_{4,1,k} &= f_2(q_{c1},q_{c2},k_1,\lambda_3,\lambda_4,\lambda_5)\cdot f_1(q_{b1},q_{b2},k_2,\lambda_1,\lambda_2,\lambda_6)\,, \\
E_{5,1,k} &= f_3(q_{b1},q_{b2},k_2,\lambda_1,\lambda_2,\lambda_5)\cdot f_3(q_{c1},q_{c2},k_1,\lambda_3,\lambda_4,\lambda_6)\,, \\
E_{6,1,k} &= f_0(q_{b1},q_{b2},\lambda_1,\lambda_2)\cdot f_4(q_{c1},q_{c2},k_1,k_2,\lambda_3,\lambda_4,\lambda_5,\lambda_6)\,, \\
E_{7,1,k} &= f_0(q_{b1},q_{b2},\lambda_1,\lambda_2)\cdot f_5(q_{c1},q_{c2},k_1,k_2,\lambda_3,\lambda_4,\lambda_5,\lambda_6)\,, \\
E_{8,1,k} &= f_0(q_{b1},q_{b2},\lambda_1,\lambda_2)\cdot f_6(q_{c1},q_{c2},k_1,k_2,\lambda_3,\lambda_4,\lambda_5,\lambda_6)\,, \\
E_{9,1,k} &= f_0(q_{b1},q_{b2},\lambda_1,\lambda_2)\cdot f_7(q_{c1},q_{c2},k_1,k_2,\lambda_3,\lambda_4,\lambda_5,\lambda_6)\,. \quad (32)
\end{aligned}
$$

Applying the exchange symmetries between the two gluons and among the quarks, the following relations may be obtained:

$$\begin{aligned}
E_{1,3,k} &= E_{4,2,k},\ E_{2,3,k} = E_{2,2,k},\ E_{3,3,k} = E_{3,2,k}\,,\\
E_{4,3,k} &= E_{1,2,k},\ E_{5,3,k} = E_{5,2,k},\ E_{1,4,k} = E_{4,1,k}\,,\\
E_{2,4,k} &= E_{2,1,k},\ E_{3,4,k} = E_{3,1,k},\ E_{4,4,k} = E_{1,1,k}\,,\\
E_{5,4,k} &= E_{5,1,k},\ E_{9,4,k} = E_{9,1,k} + E_{9,2,k} - E_{9,3,k}\,. \qquad (33)
\end{aligned}$$

Furthermore, for the diagrams involving three gluon vertices, by using a proper decomposition and the results in Tables.II and III, $E_{6,j,k}$ may be replaced as

$$\begin{aligned}
E_{6,1,k} &= E_{7,1,k} + 2q_{c2}\cdot k_2 E_{9,1,k} - E_{3,2,k} + E_{1,2,k}\,,\\
E_{6,2,k} &= E_{7,2,k} + 2q_{c2}\cdot k_1 E_{9,2,k} - E_{3,1,k} + E_{1,1,k}\,,\\
E_{6,3,k} &= E_{7,3,k} + 2q_{b2}\cdot k_2 E_{9,3,k} - E_{3,4,k} + E_{1,4,k}\,,\\
E_{6,4,k} &= E_{7,4,k} + 2q_{c2}\cdot k_1 E_{9,4,k} - E_{3,3,k} + E_{1,3,k}\,; \qquad (34)
\end{aligned}$$

and $E_{7,j,k}$ may be replaced as

$$\begin{aligned}
E_{7,1,k} &= -E_{4,1,k} + E_{2,1,k} + E_{8,1,k} - 2q_{c1}\cdot k_1(2E_{5,1,k} - 2E_{5,2,k} + E_{9,1,k})\,,\\
E_{7,2,k} &= -E_{4,2,k} + E_{2,2,k} + E_{8,2,k} - 2q_{c1}\cdot k_2(2E_{5,2,k} - 2E_{5,1,k} + E_{9,2,k})\,,\\
E_{7,3,k} &= -E_{4,3,k} + E_{2,3,k} + E_{8,3,k} - 2q_{b1}\cdot k_1(2E_{5,3,k} - 2E_{5,4,k} + E_{9,3,k})\,,\\
E_{7,4,k} &= -E_{4,4,k} + E_{2,4,k} + E_{8,4,k} - 2q_{b1}\cdot k_2(2E_{5,4,k} - 2E_{5,3,k} + E_{9,4,k})\,. \qquad (35)
\end{aligned}$$

Thus the seven kinds of basic functions $E_{m,j,k}$ ($m = 1,\cdots,5,8,9$, $j = 1,\cdots,4$, $k = 1,\cdots 64$) may be written in a very compact form. As an explicit example, $E_{m,1,1}$ ($m = 1,\cdots,5,8,9$) is shown in one of the appendices.

F. Rearrangement of the color factor for the amplitude

As shown in section II, there are only five independent color factors, and we may choose them as C_{mij} ($m = 1,\cdots,5$), where i,j $(1,2,3)$ are the indices of the final b and $\bar{c}$ quarks' colors respectively. Thus the whole amplitude may be rewritten as

$$\begin{aligned}
M^{(\lambda_1,\lambda_4,\lambda_5,\lambda_6)}(q_{b1},q_{b2},q_{c1},q_{c2},k_1,k_2) &= \sum_{i=1}^{36} M_i^{(\lambda_1,\lambda_4,\lambda_5,\lambda_6)}(q_{b1},q_{b2},q_{c1},q_{c2},k_1,k_2)\\
&= \sum_{m=1}^{5} C_{mij} M_m'^{(\lambda_1,\lambda_4,\lambda_5,\lambda_6)}(q_{b1},q_{b2},q_{c1},q_{c2},k_1,k_2)\ , \qquad (36)
\end{aligned}$$

where C_{mij} $(m = 1, \cdots, 5)$ are the five independent color factors, defined in subsection A. With Eq.(22), $M_m'^{(\lambda_1,\lambda_4,\lambda_5,\lambda_6)}(q_{b1}, q_{b2}, q_{c1}, q_{c2}, k_1, k_2)$ (in short notation M_m') can be further factorized as

$$M_m' = \sum_{\lambda_2,\lambda_3} C_{mij} M_{Fm}'^{(\lambda_1,\lambda_2,\lambda_3,\lambda_4,\lambda_5,\lambda_6)}(q_{b1}, q_{b2}, q_{c1}, q_{c2}, k_1, k_2) D_2 B_{B_c(B_c^*)}^{(\lambda_2,\lambda_3)}(q_{b2}, q_{c1}) \ , \tag{37}$$

where $M_{Fm}'^{(\lambda_1,\lambda_2,\lambda_3,\lambda_4,\lambda_5,\lambda_6)}(q_{b1}, q_{b2}, q_{c1}, q_{c2}, k_1, k_2)$ (in short notation M_{Fm}') is the amplitude of the $2 \to 4$ free quark process $gg \to c + \bar{c} + b + \bar{b}$.

Owing to the fact that each of the terms in the amplitude M_m' (M_{Fm}') is related to one of the 36 Feynman diagrams, the explicit formulae for $M_m'(M_{Fm}')$ $(m = 1, \cdots, 5)$ may be written down directly. With the nine kinds of basic functions $E_{i,m,k}$ Eqs.(32-35), M_{Fm}' may be written as

$$\begin{aligned}
M_{F1}' \ = \ & \frac{D_1}{2}\Big(2(X_{3a} + X_{4c} + X_{5b})E_{1,1,k} - 2X_{4e}E_{2,4,k} - 2X_{4c}E_{3,1,k} + 2X_{4e}E_{4,4,k} \\
& -X_{5d}(2E_{5,1,k} - 4E_{5,2,k} + E_{9,1,k} + E_{9,2,k}) + 2\{-(X_{1g} + X_{5c})E_{6,1,k} \\
& +(X_{1b} + X_{1g} + X_{5c})E_{6,2,k} + X_{5c}(E_{8,1,k} - E_{8,2,k}) - X_{2h}E_{8,3,k} + \\
& (X_{2f} + X_{2h})E_{8,4,k} + 2X_{4e}E_{5,4,k}q_{b1} \cdot k_2\} + 4X_{4c}E_{5,1,k}q_{c2} \cdot k_1 - (X_{1g} + \\
& X_{5c})(E_{9,1,k} - E_{9,2,k})f_3 + X_{5c}(4E_{5,1,k} - 4E_{5,2,k} + E_{9,1,k} - \\
& E_{9,2,k})f_4 + X_{2h}(-4E_{5,3,k} + 4E_{5,4,k} - E_{9,3,k} + E_{9,4,k})f_6 - \\
& 2X_{5b}\{E_{2,1,k} + E_{3,1,k} - E_{4,1,k} - E_{5,1,k}(s_c - s_1 + s_b)\}\Big) \ , \qquad (38) \\
M_{F2}' \ = \ & \frac{D_1}{2}\Big(2(X_{3e} + X_{4a} + X_{5a})E_{1,2,k} - 2X_{4g}E_{2,3,k} - 2X_{4a}E_{3,2,k} + \\
& 2(X_{1a} + X_{1g} + X_{5c})E_{6,1,k} - (X_{1g} + X_{5c})E_{6,2,k} + X_{5c}(E_{8,2,k} - E_{8,1,k}) + \\
& (X_{2e} + X_{2h})E_{8,3,k} - X_{2h}E_{8,4,k}) - X_{5d}(2E_{5,2,k} + E_{9,1,k} + E_{9,2,k}) + \\
& 2X_{4g}(E_{4,3,k} + 2E_{5,3,k}q_{b1} \cdot k_1) + 4X_{4a}E_{5,2,k}q_{c2} \cdot k_2 + (X_{1g} + X_{5c})(E_{9,1,k} - \\
& E_{9,2,k})f_3 + X_{5c}(4E_{5,2,k} - E_{9,1,k} + E_{9,2,k})f_4 + 4E_{5,1,k} \cdot (X_{5d} - X_{5c}f_4) + \\
& X_{2h}(4E_{5,3,k} - 4E_{5,4,k} + E_{9,3,k} - E_{9,4,k})f_6 - 2X_{5a}\{E_{2,2,k} + E_{3,2,k} - \\
& E_{4,2,k} - E_{5,2,k}(-s_2 + s_b + s_c)\}\Big) \ , \qquad (39) \\
M_{F3}' \ = \ & \frac{D_1}{2}\Big(-2(X_{4c} + X_{5b})E_{1,1,k} + 2X_{4e}E_{2,4,k} + 2(X_{3c} + X_{4c})E_{3,1,k} + \\
& 2X_{3d}E_{4,1,k} + 2(X_{5c}E_{6,1,k} - X_{5c}E_{6,2,k} + X_{2a}E_{6,4,k} + X_{2g}(-E_{6,3,k} + \\
& E_{6,4,k}) + X_{1d}E_{7,2,k} + X_{2d}E_{7,4,k} - (X_{1h} + X_{5c})E_{8,1,k} + \\
& (X_{1f} + X_{1h} + X_{5c})E_{8,2,k}) + X_{5d}(2E_{5,1,k} - 4E_{5,2,k} + E_{9,1,k} +
\end{aligned}$$

$$
\begin{aligned}
& E_{9,2,k}) - 2X_{4e}(E_{4,4,k} + 2E_{5,4,k}q_{b1}\cdot k_2) - 4X_{4c}E_{5,1,k}q_{c2}\cdot k_1 \\
& + X_{5c}(E_{9,1,k} - E_{9,2,k})f_3 - (X_{1h} + X_{5c})(4E_{5,1,k} - 4E_{5,2,k} + \\
& E_{9,1,k} - E_{9,2,k})f_4 - X_{2g}(E_{9,3,k} - E_{9,4,k})f_5 + 2\{(X_{3b} + X_{5b})E_{2,1,k} + \\
& X_{5b}[E_{3,1,k} - E_{4,1,k} - E_{5,1,k}(-s_1 + s_b + s_c)]\}\Big), \qquad (40) \\
M'_{F4} \;=\; & \frac{D_1}{2}\Big(-2(X_{4a} + X_{5a})E_{1,2,k} + 2(X_{3g} + X_{4a})E_{3,2,k} + 2X_{3h}E_{4,2,k} - \\
& 2X_{5c}E_{6,1,k} + 2(X_{5c}E_{6,2,k} + (X_{2a} + X_{2g})E_{6,3,k} - X_{2g}E_{6,4,k} + \\
& X_{1c}E_{7,1,k} + X_{2c}E_{7,3,k} + (X_{1e} + X_{1h} + X_{5c})E_{8,1,k} - (X_{1h} + X_{5c})E_{8,2,k}) + \\
& X_{5d}(2E_{5,2,k} + E_{9,1,k} + E_{9,2,k}) + 2X_{4g}(E_{2,3,k} - E_{4,3,k} - \\
& 2E_{5,3,k}q_{b1}\cdot k_1) - 4X_{4a}E_{5,2,k}q_{c2}\cdot k_2 - X_{5c}(E_{9,1,k}E_{9,2,k})f_3 - \\
& -(X_{1h} + X_{5c})(4E_{5,2,k} - E_{9,1,k} + E_{9,2,k})f_4 + 4E_{5,1,k}(-X_{5d} + \\
& (X_{1h} + X_{5c})f_4) + X_{2g}(E_{9,3,k} - E_{9,4,k})f_5 + 2\{(X_{3f} + X_{5a})E_{2,2,k} + \\
& X_{5a}[E_{3,2,k} - E_{4,2,k} - E_{5,2,k}(-s_2 + s_b + s_c)]\}\Big), \qquad (41) \\
M'_{F5} \;=\; & D_1\Big(-(X_{5b}E_{1,1,k}) + (X_{4d} + X_{5b})E_{2,1,k} - (X_{3d} + X_{4d})E_{4,1,k} - X_{3h}E_{4,2,k} - \\
& X_{2a}(E_{6,3,k} + E_{6,4,k}) - X_{1e}E_{8,1,k} - X_{1f}E_{8,2,k} - X_{5d}(E_{5,1,k} + E_{5,2,k} \\
& - E_{9,1,k} - E_{9,2,k}) + X_{4h}(-E_{1,3,k} + E_{3,3,k} - 2E_{5,3,k}q_{b2}\cdot k_1) + \\
& X_{4f}(-E_{1,4,k} + E_{3,4,k} - 2E_{5,4,k}q_{b2}\cdot k_2) - 2X_{4d}E_{5,1,k}q_{c1}\cdot k_1 + \\
& X_{4b}(E_{2,2,k} - E_{4,2,k} - 2E_{5,2,k}q_{c1}\cdot k_2) - X_{5b}(-E_{3,1,k} + E_{4,1,k} + \\
& E_{5,1,k}(-s_1 + s_b + s_c)) - X_{5a}\{E_{1,2,k} - E_{2,2,k} - E_{3,2,k} + \\
& E_{4,2,k} + E_{5,2,k}(-s_2 + s_b + s_c)\}\Big), \qquad (42)
\end{aligned}
$$

where X_i are the scalar factors of the propagators, labelled by the corresponding Feynman diagram, $s_1 = (k_1 - q_{b1} - q_{b2})^2$, $f_5 = 2k_1\cdot k_2 - 2q_{b2}\cdot k_1 - 2q_{b2}\cdot k_2$ and $f_6 = 2k_1\cdot k_2 - 2q_{b1}\cdot k_1 - 2q_{b1}\cdot k_2$.

G. Programme check for the subprocess $gg \to B_c(B_c^*) + b + \bar{c}$ and hadronic production of B_c

With all the above preparations, it is straightforward to write the programme for computing the cross section of the subprocess. Applying the pQCD factorization theorem, various cross sections of the $B_c(B_c^*)$-hadronic production may be obtained by integrating the hadron structure functions over the cross section of the subprocess $gg \to B_c(B_c^*) + b + \bar{c}$.

Various cross-sections of the subprocess $gg \to B_c(B_c^*) + b + \bar{c}$ may be calculated, once the amplitude (with initial state color factors averaged and final state color factors summed up) has been computed. One only has to integrate over the proper phase space according to the requirements. Since the final state of the process is a massive three-body state, the phase space integrations are carried out numerically. As in the more general case, a Monte-Carlo simulation integration over the phase space is a practical solution, when one is averaging over the helicities of the initial gluons and spins of the quarks (and spins of B_c^* if $gg \to B_c^* + b + \bar{c}$ is considered). To do the phase space integration, we first use the routine RAMBOS [26] to generate the requested phase space points (the energy-momentum conservation is guaranteed and some additional constraints for specific requests are matched). We then use the VEGAS [27] program (with necessary revisions to suit the present problem) to perform the integrations. The VEGAS program is useful for obtaining accurate total cross-sections, smooth distributions for the $p_{\rm T}$[32] and the rapidity Y of the B_c-meson, and so on. When running VEGAS, the most important samples for the matrix element squared are taken first. Then by taking an adequate number of points for the integration, we obtain a final result, which is stable with respect to increasing the number of points and compatible with the requested statistical error.

To check the program, we calculate the total cross-section of the subprocess, $gg \to B_c(B_c^{(*)}) + b + \bar{c}$, as well as the B_c $p_{\rm T}$ and Y distributions for various subprocess center-of-mass energies, using the same parameters (*e.g.* α_s, m_b, m_c, m_{B_c} and $f_{B_c(B_c^*)}$) as in Refs.[7, 8]. The results are compared with those in Refs.[7, 8] and shown in Table IV and Table V. The B_c-$p_{\rm T}$ and B_c-Y distributions for various subprocess center-of-mass energies are compared with Ref.[7] and shown in Fig.9. The integrated cross sections versus the center-of-mass energy of the subprocess for a fixed value of $\alpha_s = 0.2$ are also shown in Fig.10. One may see the agreement between our results and those in Ref.[7, 8] from the tables and figures. Since the present programme and that used in Ref.[7, 8] are totally different, the agreement is a very solid check for both of them.

According to pQCD, the production cross section is formulated

$$d\sigma = \sum_{ij} \int dx_1 \int dx_2 F_{H_1}^i(x_1, \mu_F) \times F_{H_2}^j(x_2, \mu_F) d\hat{\sigma}_{ij \to B_c X}(x_1, x_2, \mu_F), \tag{43}$$

where $F^i(x, \mu_F)$ is this distribution function of the parton i in the hadron H, $d\hat{\sigma}_{ij \to B_c X}(x_1, x_2, \mu_F)$ is the cross section for the relevant inclusive production (i+$j \to B_c$+X).

TABLE IV: Comparison of total cross sections for $gg \to B_c(B_c^*) + b + \bar{c}$ with the corresponding results of Ref.[7]. The input parameters are $m_b = 4.9$ GeV, $m_c = 1.5$ GeV, $M_{B^*c} = m_b + m_c$, $f_{Bc} = 0.480$ GeV, $\alpha_s = 0.2$. The number in parenthesis shows the Monte Carlo uncertainty in the last digit. The cross sections are expressed in nb.

$\sqrt{\bar{s}}$	20 GeV	30 GeV	60 GeV
σ_{B_c}	$0.6579(5) \times 10^{-2}$	$0.9465(8) \times 10^{-2}$	$0.7872(8) \times 10^{-2}$
σ_{B_c}[7]	$0.661(7) \times 10^{-2}$	$0.949(8) \times 10^{-2}$	$0.782(9) \times 10^{-2}$
$\sigma_{B_c^*}$	$0.1606(1) \times 10^{-1}$	$0.2460(3) \times 10^{-1}$	$0.2033(2) \times 10^{-1}$
$\sigma_{B_c^*}$[7]	$0.160(2) \times 10^{-1}$	$0.244(3) \times 10^{-1}$	$0.203(3) \times 10^{-1}$

TABLE V: Comparison of total cross sections for $gg \to B_c + b + \bar{c}$ with the corresponding results of Ref[8]. The input parameters are $m_b = 3m_c$, $M_{B_c} = 6.30GeV$, $f_{Bc} = 0.480GeV$, $\alpha_s = 0.2$. The number in parenthesis shows the Monte Carlo uncertainty in the last digit. The cross sections are expressed in nb.

$\sqrt{\bar{s}}$	20 GeV	30 GeV	60 GeV	80 GeV
σ_{B_c}	$0.6853(5) \times 10^{-2}$	$0.9731(8) \times 10^{-2}$	$0.7997(9) \times 10^{-2}$	$0.6244(9) \times 10^{-2}$
σ_{B_c}[8]	$0.686(2) \times 10^{-2}$	$0.971(4) \times 10^{-2}$	$0.793(5) \times 10^{-2}$	$0.623(5) \times 10^{-2}$

With the pQCD factorization formula Eq.(43), various cross sections for the hadronic production of the meson $B_c(B_c^*)$ can be computed by integrating over two more dimensions of the structure functions of the incoming hadrons.

The programme for the hadronic production of the $B_c(B_c^*)$ mesons has also been checked by evaluating the hadronic production of B_c at Tevatron. The explicit example is to produce the B_c meson by using the next to leading order running α_s, the characteristic energy scale $Q^2 = \bar{s}/4$ (NQ2=1) of the production and the CTEQ3M set of parton distribution functions. The results for the distributions and the cross sections agree with those in Ref.[8].

III. THE PROGRAMME: BCVEGPY GENERATOR

The programme BCVEGPY is a generator for hadronic production of B_c mesons in form of a Fortran package, based on the dominant subprocess $gg \to B_c(B_c^*)+b+\bar{c}$. Concerning its implementation in PYTHIA, BCVEGPY is written in the same format as in PYTHIA (including common block variables). Thus it is easy to implement straightforward in PYTHIA as an external process, and in this way all the functions of PYTHIA can be utilized in connection with the use of BCVEGPY.

A. Structure of the program

The BCVEGPY Fortran package contains five files: bcvegpy.for, genevnt.for, sqamp.for, foursets.for and pythia6208.for. The routine bcvegpy.for is the main program of BCVEGPY which takes care of the necessary input parameters for the event generation and outputs a variety of results, such as the distribution of the transverse momentum $p_{\rm T}$ and rapidity Y of the produced B_c, *etc.*. In the routine genevnt.for, there is a function TOTFUN and five subroutines: EVNTINIT, UPINIT, UPEVNT, BCPYTHIA and PHPOINT. The subroutines EVNTINIT and UPINIT are used for initializing the parameters when running BCVEGPY in the PYTHIA environment. The event generation starts by calling PYEVNT (a PYTHIA routine) just after calling the subroutines EVNTINIT and UPINIT. The routine UPEVNT (a PYTHIA user routine) is then called, that allows the implementation of an external processes. The functioning of the subroutine UPEVNT is determined by an input flag, which is a number read in from the file input.dat. When the input flag switches on, the generation of complete events may be carried out. UPEVNT calls the subroutine BCPYTHIA and the full information, *i.e.* the status code, the mother code, the color flow *etc.* for the final state particles ($B_c(B_c^*)$ meson and two jets b and $\bar{c}$). The allowed phase-space for the production (*i.e.* energy-momentum consevation) controls the production completely. The phase-space is generated by calling the subroutine PHPOINT. The function TOTFUN computes the value of the integrand for the phase space integration by calling the subroutine AMP2UP which is in sqamp.for. The subroutine AMP2UP is written according to the techniques described in the previous sections and its purpose is to compute the square of the amplitude for the hard subprocess $gg \to B_c(B_c^*) + b + \bar{c}$. In files sqamp.for and foursets.for, there are quite a

lot subroutines and functions, that are needed for calculating the square of the amplitude. All of them will be explained in Appendix C. When running the package BCVEGPY, the PYTHIA library must be linked; in particular, the generator is designed to be interfaced to the PYTHIA version 6.2[25]. For reference, we include the file pythia6208.for in our package. In order to increase the phase space integration accuracy, one may apply the subroutine VEGAS (in sqamp.for) to optimize the sampling of the phase space points for phase space integration before calling PYTHIA.

B. Use of the generator

BCVEGPY can be used for generating a huge sample of $B_c(B_c^*)$ meson for hadronic collisions efficiently (based on the mechanism with $gg \to B_c(B_c^*) + b + \bar{c}$ as the main subprocess). Furthermore, if the generator is implemented in PYTHIA, a complete event with two hadronized quark jets and a decayed $B_c(B_c^*)$ meson can be simulated. If one would like to simulate only the hadronic production of the $B_c(B_c^*)$ meson, BCVEGPY alone is sufficient. Furthermore, users may choose either the hadronic production or the subprocess $gg \to B_c(B_c^*) + b + \bar{c}$ only, just by setting the value of the flag ISUBONLY equal to 0 to switch on the integration for the parton distribution (structure) functions, or setting the flag equal to 1 for the subprocess only. Since the cross section of B_c production in hadron collisions is small compared to the B^+, B^0, B_s production, the efficiency for producing B_c events through fragmentation of a $\bar{b}$ quark, as done in the standard PYTHIA, is too low (the ratio of the signal to the background is too small). For experimental feasibility studies of B_c mesons, a very large sample of B_c events is needed. Therefore BCVEGPY, which is powerful for generating B_c events only with full information in hadron-hadron collision, is very useful.

Users may communicate with or give instructions to the program through an input file (input.dat). The output files include 1s0.dat (the B_c total cross-section) or 3s1.dat (the B_c^* total cross-section); pt.dat (the B_c-$p_{\rm T}$ distribution); shat.dat (the B_c-$\sqrt{\hat{s}}$ distribution); rap.dat (the B_c-Y rapidity distribution); pseta.dat (the B_c-η pseudorapidity distribution) and grade.dat (the sampling importance function obtained by VEGAS). The input.dat file allows users to setup the generation parameters and requests, while the output files collect the relevant event information.

TABLE VI: The parameter values in the sequential order in the input.dat file.

PMBC PMB PMC FBC
PTCUT ETACUT ECM IBCSTATE IGENERATE IVEGASOPEN
NUMBER NITMX
NQ2 NPDFU NEV
ISHOWER MSTP(51)
IDWTUP MSTU(111) PARU(111)
ISUBONLY SUBENERGY IGRADE

The sequential order and the format of the parameters in the file input.dat should be the same as in the Table VI. The parameters specified in the input file are:

• PMBC, PMB, PMC=: masses of the B_c meson, b quark and c quark respectively (in units GeV);

• FBC=: decay constant for the B_c meson (in units GeV);

• PTCUT=: $p_{\rm T}$ cut for the $B_c(B_c^*)$ meson (in units GeV, value can be freely selected by users);

• ETACUT=: Y cut for the $B_c(B_c^*)$ meson (value can be freely selected by the users);

• ECM=: total energy for the hadron collision (in units GeV);

• IBCSTATE=: state of the $B_c(B_c^*)$ meson: IBCSTATE=1 for $B_c[1^1S_0]$ and IBCSTATE=2 for $B_c^*[1^3S_1]$;

• IGENERATE=: whether to generate complete events. IGENERATE=0, when users wish the simulation to stop after the generation of the 'final state' containing the B_c meson, b-jet and $\bar{c}$-jet of the subprocess $gg \to B_c + b + \bar{c}$; IGENERATE=1, when users wish that complete events including the B_c production are to be generated. In the latter case, IDWTUP=1;

• IVEGASOPEN=: whether switch on/off the VEGAS subroutine: IVEGASOPEN=1 for using VEGAS; IVEGASOPEN=0 for not using VEGAS;

• NUMBER=: total number of times for calling the integrand (VEGAS parameter, see VEGAS manual). The parameter is needed only when IVEGASOPEN=1 in each iteration;

• NITMX=: upper limit for the number of iterations (VEGAS parameter, see VEGAS manual). The parameter is needed only when IVEGASOPEN=1;

• NQ2=: choice of Q^2, the type of the characteristic energy scale squared in the production

(in units GeV^2). Here seven choices are available: i). NQ2=1: $Q^2 = \bar{s}/4$ ($\bar{s}$ is the squared center-of-mass energy of the subprocess); ii). NQ2=2: $Q^2 = \bar{s}$; iii). NQ2=3: $Q^2 = p_{TB_c}^2 + m_{B_c}^2$; iv). NQ2=4: $Q^2 = (\sqrt{p_{TB_c}^2 + m_{B_c}^2} + \sqrt{p_{Tb}^2 + m_b^2} + \sqrt{p_{Tc}^2 + m_c^2})^2$; v). NQ2=5: $Q^2 = (\sqrt{p_{TB_c}^2 + m_{B_c}^2} + \sqrt{p_{Tb}^2 + m_b^2} + \sqrt{p_{Tc}^2 + m_c^2})^2/9$; vi). NQ2=6: $Q^2 = p_{Tb}^2 + m_b^2$ for the α_s in parton distribution functions and in the coupling to the b-quark line, and $Q^2 = 4m_c^2$ for the α_s in the coupling to the $\bar{c}$-quark line; vii). NQ2=7: $Q^2 = p_{Tb}^2 + m_b^2$;

• NPDFU=: choice of the collision type of hadrons. The assignments can be found in PYTHIA manual, *e.g.* NPDFU=1 for $p - \bar{p}$ and NPDFU=2 for $p - p$;

• NEV=: number of the events for the hadronic production $h + h \to B_c + \cdots$ (h means a hadron) to be generated;

• ISHOWER=: whether to switch on/off the showers, including initial and final states, multiple interactions, hadronization; *e.g.* ISHOWER=1 for 'on' and ISHOWER=0 for 'off' (see PYTHIA manual);

• MSTP(51)=: choice of the proton parton-distribution set; *e.g.* MSTP(51)=2 for CTEQ3M; MSTP(51)=7 for CTEQ5L; MSTP(51)=8 for CTEQ5M *etc.* (PYTHIA parameter, see PYTHIA manual);

• IDWTUP=: master switch dictating how the event weights and the cross-sections should be interpreted (PYTHIA parameter, see PYTHIA manual); *e.g.* when IDWTUP=1, parton-level events have a weight at the input to PYTHIA. Events are then either accepted or rejected, so that fully generated events at the output have a common weight; when IDWTUP=3, parton-level events have a unit weight at the input to PYTHIA *i.e.* they are always accepted;

• MSTU(111)=: order of α_s in the evaluation in PYALPS (a PYTHIA routine for calculating α_s, see PYTHIA manual); *e.g.* MSTU(111)=1 for leading order (LO); MSTU(111)=2 for next leading order (NLO);

• PARU(111)=: constant value of α_s (see PYTHIA manual), which is used only when MSTU(111)=0;

• ISUBONLY=: whether to keep the information only of the sub-process $gg \to B_c(B_c^*)+b+\bar{c}$; ISUBONLY=0 for the full hadronic production, *i.e.* the structure functions are connected; ISUBONLY=1 for the subprocess only.

• SUBENERGY=: the energy (in units GeV) of the sub-process $gg \to B_c(B_c^*) + b + \bar{c}$. It is needed only when ISUBONLY=1;

• IGRADE=: whether to use the grade generated by previous running VEGAS when IVEGASOPEN=0; IGRADE=1 means to use; IGRADE=0 means not to use.

In the package, two subroutines PHASE-GEN and VEGAS are needed when integrating over the phase space:

The subroutine PHASE-GEN(YY,ET,WT)

The subroutine is included in the file sqamp.for and is called by another subroutine PHPOINT in genevnt.for. The purpose is to evaluate the allowed phase-space points for the sub-process $gg \to B_c(B_c^*) + b + \bar{c}$ when the center-of-mass energy of the sub-process is fixed, and to return a non-zero weight for each allowed phase space point. The energy-momentum conservation is integrated out in order to reduce the dimension of the phase space integration by four. Since the subprocess is a three body final state, the nine-dimensional phase space integration of the process turns into a five-dimensional one with a proper Jacobi determinant, when PHASE-GEN has been applied.

The variables in the routine are:

• YY(5)=: a five-dimensional random number with a range from 0 to 1 for each dimension, corresponding to the five independent integration variables for the phase-space;

• ET=: center-of-mass energy for the subprocess (in units GeV); ET can be chosen freely when ISUBONLY=1, otherwise when ISUBONLY=0, ET is determined by PHPOINT;

• WT=: the returned weight for each generated phase-space point.

The subroutine VEGAS(FXN,NDIM,NCALL,ITMX,NPRN)

• FXN=: the integrand calling the function TOTFUN in genevnt.for;

• NDIM=: number of integration dimensions for the generator; NDIM=5 when ISUBONLY=1; NDIM=7 when ISUBONLY=0;

• NCALL=: maximum total number of the times to call the integrand in each iteration set by the user;

• ITMX=: maximum number of allowed iterations set by the user;

• NPRN=: print out level; (see VEGAS manual) *e.g.* NPRN=2, when printing out only the cross section values and errors.

Note that the units of all the output data is well explained in the programme.

TABLE VII: Generation parameters used in the sample generation.

..... INITIAL PARAMETERS .....
Bc IN 1^1S_0
GENERATE EVNTS 30000000 FOR TEVATRON ENERGY(GEV) $0.20E+04$
M_{Bc}=6.400 M_{B}= 4.900 M_{C}=1.500 f_{Bc}=0.4800
Q2 TYPE= 1 ALPHAS ORDER= 2
PARTON DISTRIBUTION FUNCTION: CTEQ 3M
USING PYTHIA MODEL FOR IDWTUP= 3
PTCUT =0.000 GeV
NO RAPIDITY CUT
USING VEGAS: NUMBER IN EACH ITERATION= 300000 ITERATION= 27
..... END OF INITIALIZATION .....

C. Generator checks

The whole Fortran package is checked by examining the gauge invariance of the amplitude. The matrix element vanishes when the polarization vector of an initial gluon is substituted by the momentum vector of this gluon.

For further checking, we have performed several test runs. By setting the parameter ISUBONLY=1 in the input.dat file, we obtain the transverse momentum $p_{\rm T}$ and rapidity Y distributions for the produced B_c, and the total cross-section for the sub-process $gg \to B_c(B_c^*) + b + \bar{c}$. The results, which are shown in the previous section, coincide well with several groups' results[8].

When running the programme, the initialization is shown as a screen snap-shot in Table VII. Some output data are shown by Figs.11,12.

IV. CONCLUSIONS

A B_c meson generator BCVEGPY for hadronic collisions, based on the dominant subprocess $gg \to B_c(B_c^*) + b + \bar{c}$, has been developed and well-tested. The generator has been interfaced with PYTHIA, which takes care of producing the full event and filling the

standard PYTHIA event common block. In view of the prospects for B_c physics at Tevatron and at LHC, the generator offers a valuable platform for further experimental studies.

Acknowledgement: The author (C.-H. Chang) would like to thank Lund University for warm hospitality during his visit. The authors would like to thank Dr. Y.-Q. Chen and Mr. Y.-B. Sun for useful discussions, and Prof. T. Sjöstrand for valuable advice and comments. The work was supported in part by Nature Science Foundation of China (NSFC).

---

[1] CDF Collaboration, F. Abe *et al.*, Phys. Rev. **D58**, 112004 (1998).

[2] K. Anikeev *et al.*, hep-ph/0201071.

[3] Chao-Hsi Chang, Talk in *ATLAS Physics Workshop* 12-16 Sept. 2001, at Lund University; *Proceedings of the XXXVIIth RENCONITRES DE MORIOND* Les Arcs, Savoie, France, **2002 QCD and High Energy Hadronic Interactions**, p-27, hep-ph/20205112.

[4] C. Quigg, *Proceedings of the Workshop on B Physics at Hadron Accelerators*, Snowmass (CO) USA, 1993, Eds. P. McBride and C.S. Mishra.

[5] Chao-Hsi Chang and Yu-Qi Chen, Phys. Rev. D **46**, 3854 (1992); Erratum Phys. Rev. **50**, 6013 (1994).

[6] E. Braaten, K. Cheung and T.C. Yuan, Phys. Rev. D **48**, 4230 (1993); E. Braaten, K. Cheung and T.C. Yuan, Phys. Rev. D **48**, R5049 (1993).

[7] Chao-Hsi Chang and Yu-Qi Chen, Phys. Rev. D **48**, 4086 (1993).

[8] Chao-Hsi Chang, Yu-Qi Chen, Guo-Ping Han and Hung-Tao Jiang, Phys. Lett. B **364**, 78 (1995); Chao-Hsi Chang, Yu-Qi Chen and R. J. Oakes, Phys. Rev. D **54**, 4344 (1996); K. Kolodziej, A. Leike and R. Rückl, Phys. Lett. B **355**, 337 (1995).

[9] A.V. Berezhnoy, V.V. Kiselev, A.K. Likhoded, Z. Phys. A **356**, 79 (1996); S.P. Baranov, Phys. Rev. D **56** 3046, (1997).

[10] K. Cheung, Phys. Lett. B **472**, 408 (2000).

[11] Yu-Qi Chen and Yu-Ping Kuang, Phys. Rev. D **46**, 1165 (1992); E. Eichten, C. Quigg, Phys.

Rev. D **49** 5845 (1994); Phys. Rev. D **52**, 1726 (1995); S.S. Gershtein, V.V. Kiselev, A.K. Likhoded and A.V. Tkabladze, Phys. Rev. D **51**, 3613 (1995).

[12] Chao-Hsi Chang, Yu-Qi Chen, Phys. Rev. **D49**, 3399 (1994); Chao-Hsi Chang and Yu-Qi Chen, Commun. Theor. Phys. **23** (1995) 451.

[13] A. Abd El-Hady, J.H. Munoz and J.P. Vary, Phys. Rev. D**62** 014014 (2000).

[14] N. Isgur, D. Scora, B. Grinstein and M. Wise, Phys. Rev. D **39**, 799 (1989); M. Lusignoli and M. Masetti, Z. Phys. C **51**, 549 (1991); D. Scora and N. Isgur, Phys. Rev. D **52**, 2783 (1995). Dongsheng Du, G.-R. Lu and Y.-D. Yang, Phys. Lett. B **387**, 187 (1996); Dongsheng Du *et al.*, Phys. Lett. B **414**, 130(1997); Jia-Fu Liu and Kuang-Ta Chao, Phys. Rev. D **56** 4133, (1997); P. Colangelo and F.De Fazio, Phys. Rev. D **61** 034012 (2000). V.V. Kiselev, A.E. Kovalsky and A.K. Likhoded, Nucl. Phys. B **585** 353 (2000); V.V. Kiselev, A.K. Likhoded and A.I. Onishchenko, Nucl. Phys. B **569** 473, (2000). M.A. Nobes and R.M. Woloshyn, J. Phys. G **26** 1079, (2001).

[15] Chao-Hsi Chang, Shao-Long Chen, Tai-Fu Feng and Xue-Qian Li, Phys. Rev. D **64**, 014003 (2001); Commun. Theor. Phys. **35**, 51 (2001).

[16] M. Beneke and G. Buchalla, Phys. Rev. D **53**, 4991 (1996).

[17] Chao-Hsi Chang, J.-P. Cheng and C.-D. Lü, Phys. Lett. **B 425**, 166 (1998); P. Colangelo and F. De Fazio, Mod. Phys. Lett. **A 14**, 2303 (1999); Chao-Hsi Chang, Cai-Dian Lü, Guo-Li Wang and Hong-Shi Zong, Phys. Rev. **D60** 114013, 1999; Chao-Hsi Chang, Yu-Qi Chen, Guo-Li Wang and Hong-Shi Zong, Phys. Rev. D **65**, 014017 (2001); Commun. Theor. Phys. **35**, 395 (2001); Chao-Hsi Chang, Anjan K. Giri, Rukmani Mohanta and Guo-Li Wang, J. Phys. G **28**, 1403, (2002), hep-ph/0204279; Xing-Gang Wu, Chao-Hsi Chang, Yu-Qi Chen and Zheng-Yun Fang, Phys. Rev. D, **67**, 0704XX, (2003), hep-ph/0209125.

[18] J.D. Bjorken and M.C. Chen, Phys. Rev.**154**, 1534(1967).

[19] P.De Causmaecker, R. Gastmans, W. Troosts and T.T. Wu, Phys. Lett. B, **105**(1981)215; Nucl. Phys. B, **206** (1982) 53.

[20] F.A. Berends, R. Kleiss, P.D. Causmaecker, R. Gastmans, W. Troosts and T.T. Wu, Nucl. Phys. B, **206** (1982) 61; Nucl. Phys. B, **239** (1984) 382; Nucl. Phys. B, **239** (1984) 395; Nucl. Phys. B, **264** (1986) 243; Nucl. Phys. B, **264** (1986) 265.

[21] Zhan Xu, Da-Hua Zhang and Lee Chang, Nucl. Phys. B, **B291** (1987) 392.

[22] A. Ballestrero, E. Maina, hep-ph/9405384; hep-ph/9404223.

[23] L.J. Dixon, hep-ph/9601359.

[24] Hidekazu Tanaka, Comput. Phys. Commun, **48** (1998) 335.

[25] T. Sjostrand, Comput. Phys. Commun. **82** (1994) 74.

[26] R. Kleiss and W.J. Stirling, Comput. Phys. Commun, **40**(1986)359

[27] G.P. Lepage, J. Comp. Phys **27**(1978) 192

[28] Based on the potential model for heavy quarks, the ground state of the $(c\bar{b})$ bound system is in $1,^1S_0$, and according to PDG it is denoted by B_c. The first excited state $1,^3S_1$ is due to the spin-splitting (spin-spin interaction) and it is denoted by B_c^* throughout the paper. Since the spin-splitting is small, the available energy of the decays from B_c^* to B_c is so small that only dipole magnetic moment transition (M1) is allowed between them.

[29] In literature there are calculations on the hadronic production of the B_c meson with the same approach, but the computer programs have not been published (or not easy to find), so we would like to present ours by re-writing the program and comparing it with others.

[30] The CALKUL technique is essentially based on the chirality of massless fermions. Since in the massless case the chirality is equivalent to the helicity with one-to-one correspondence, in the references the authors use the term 'helicity' without ambiguity. While in this paper we adopt some techniques of CALKUL, we will frequently use 'helicity' but not 'chirality', because we consider massive fermions here.

[31] According to the non-relativistic QCD (NRQCD), although there may be non-color-singlet components for the physical B_c meson, with such small components one cannot find a subprocess in an order lower in pQCD for the B_c hadronic production. This is contrary to the case of J/ψ production (J/ψ has a hidden flavor, while the B_c has explicit flavors). Therefore it is certain that the subprocess is dominant.

[32] $p_{\rm T}$ is the transverse momentum with respect to the beam direction.

APPENDIX A: THE HELICITY FUNCTIONS FOR THE AMPLITUDE

In this Appendix, we show an example how to calculate the functions $E_{m,j,k}$.

For evaluating the inner product $\langle p\cdot q\rangle$, we introduce the notations k_+, $k_\perp$ for a light-like

momentum k^μ and use the Weyl representation for γ- matrices:

$$\gamma^0 = \begin{pmatrix} 0 & \mathbf{1} \\ \mathbf{1} & 0 \end{pmatrix}\,,\ \gamma^i = \begin{pmatrix} 0 & -\sigma^i \\ \sigma^i & 0 \end{pmatrix}\,,\ (i=1,2,3) \tag{A1}$$

with Pauli matrices

$$\sigma^1 = \begin{pmatrix} 0 & 1 \\ 1 & 0 \end{pmatrix}\,,\ \sigma^2 = \begin{pmatrix} 0 & -i \\ i & 0 \end{pmatrix}\,,\ \sigma^3 = \begin{pmatrix} 1 & 0 \\ 0 & -1 \end{pmatrix}\,, \tag{A2}$$

and

$$k_\pm = k_0 \pm k_z,\ k_\perp = k_x + ik_y = |k_\perp| e^{i\varphi_k} = \sqrt{k_+ k_-}\, e^{i\varphi_k}\,, \tag{A3}$$

where $\mathbf{1}$ is the 2×2 unit matrix and σ^i (i=1,2,3) are the Pauli matrices. Note that here we always have $k_+ \geq 0, k_- \geq 0$, because $k_+k_- \equiv k_0^2 - k_z^2 = k_x^2 + k_y^2 \geq 0$ due to $k^2 = k_0^2 - k_z^2 - k_x^2 - k_y^2 = 0$. By suitable choice of the phase we introduce the Weyl spinors

$$|k_+\rangle = \begin{pmatrix} \sqrt{k_+} \\ \sqrt{k_-}e^{i\varphi_k} \\ 0 \\ 0 \end{pmatrix},\ |k_-\rangle = \begin{pmatrix} 0 \\ 0 \\ \sqrt{k_-}e^{-i\varphi_k} \\ -\sqrt{k_+} \end{pmatrix}\,, \tag{A4}$$

and

$$\begin{aligned} \langle k_1 \cdot k_2 \rangle &= \langle k_{1-}|k_{2+}\rangle = \sqrt{k_{1-}k_{2+}}e^{i\varphi_1} - \sqrt{k_{1+}k_{2-}}e^{i\varphi_2} \\ &= k_{1\perp}\sqrt{\frac{k_{2+}}{k_{1+}}} - k_{2\perp}\sqrt{\frac{k_{1+}}{k_{2+}}}\,, \end{aligned} \tag{A5}$$

which appear to be explicitly antisymmetric. For the spinor product $\langle k_{1+}|\not{k}_3|k_{2+}\rangle$, where $k_i^2 = 0$ $(i=1,2,3)$,

$$\begin{aligned} \langle k_{1+}|\not{k}_3|k_{2+}\rangle &= \langle k_{1+}|k_{3-}\rangle\langle k_{3-}|k_{2+}\rangle \\ &= \frac{1}{\sqrt{k_{1+}k_{2+}}}(k_{1+}k_{2+}k_{3-} - k_{1+}k_{2\perp}k_{3\perp}^* - k_{1\perp}^* k_{2+}k_{3\perp} + k_{1\perp}^* k_{2\perp}k_{3+})\,, \end{aligned} \tag{A6}$$

and for the spinor product involving the polarization vector $\epsilon(s_z)$ of B_c^*,

$$\begin{aligned} \langle q_{0+}|\not{\epsilon}(s_z)\not{P}'|q_{0-}\rangle &= P'_+\epsilon(s_z)_- q_{0\perp}^* - (P'_\perp)^* q_{0+}\epsilon(s_z)_- - P'_+\epsilon(s_z)_\perp \frac{q_{0\perp}^2}{q_{0+}} + \epsilon(s_z)_\perp (P'_\perp)^* q_{0\perp}^* - \\ &\quad P'_\perp \epsilon(s_z)_\perp^* q_{0\perp}^* + q_{0+}\epsilon_\perp^* P'_- + \epsilon(s_z)_+ P'_\perp \frac{q_{0\perp}^2}{q_{0+}} - \epsilon(s_z)_+ P'_- q_{0\perp}^*\,, \end{aligned} \tag{A7}$$

where $P' = P - \frac{P^2}{2P\cdot q_0} q_0$.

Since the spinor products and the double inner spinor products are used frequently in the program, we take y_i $(i = 1, \cdots, 42)$ to denote all the possible spinor products appearing in the computation, *e.g.* $y_1 = \langle k_{1+}|\not{q}'_{c2}|q_{0+}\rangle$ and x_1, x_2 to denote the double inner spinor products:

$$x_1 = \langle q_0 \cdot k_1\rangle\langle q_0 \cdot k_2\rangle, \quad x_2 = \langle q_0 \cdot k_1\rangle^*\langle q_0 \cdot k_2\rangle^* . \tag{A8}$$

To simplify the results, we have introduced the light-like momenta q'_{b1}, q'_{b2}, q'_{c1} and q'_{c2} in terms of time-like momenta q_{b1}, q_{b2}, q_{c1} and q_{c2} respectively:

$$\begin{aligned} q'_{b1} &= q_{b1} - \frac{q_{b1}^2}{2q_{b1}\cdot q_0}q_0\,, \quad q'_{b2} = q_{b2} - \frac{q_{b2}^2}{2q_{b2}\cdot q_0}q_0\,, \\ q'_{c1} &= q_{c1} - \frac{q_{c1}^2}{2q_{c1}\cdot q_0}q_0\,, \quad q'_{c2} = q_{c2} - \frac{q_{c2}^2}{2q_{c2}\cdot q_0}q_0\,. \end{aligned} \tag{A9}$$

When the functions $E_{m,1,k}$ $(m = 1, \cdots, 5, 8, 9;\ k = 1, \cdots, 64)$ are given, $E_{m,j,k}$ $(j = 2, \cdots, 4)$ can be obtained by interchanging the initial gluon momenta and the final quark flavors. As shown below, due to the properties of the helicities, the functions may be simplified, and may even become zero for some helicities. Here we list $E_{m,1,1}$ $(m = 1, \cdots, 5, 8, 9)$ for an explicit example,

$$\begin{aligned} E_{1,1,1} &= \frac{4y_1}{x_1}\Big({m_b}^2((y_{11}-y_{12})y_{19}y_{27} + y_{10}(y_{34}y^c_{34} - y_5y^c_5)) \\ &+ y_{10}(y_{20}(y_2y^c_5 - y^c_{24}y^c_{34}) + {m_c}^2y_{35}y^c_{35})\Big)\,, \\ E_{2,1,1} &= \frac{-4}{x_1}\Big({m_b}^2y_9(y_{11}y_{19}y_{27} + y_{10}y_{34}y^c_{34}) \\ &+ y_{10}\{-(y_9y_{20}y^c_{24}y^c_{34}) + {m_c}^2(y_2y_{29}y_{31} + y_9y_{35}y^c_{35})\}\Big)\,, \\ E_{3,1,1} &= \frac{4y_1y_{16}}{x_1}\Big((({m_c}^2y_{17} - y_{11}y_{32})y^c_{17} + {m_b}^2(y_5y^c_5 - y_{34}y^c_{34}) \\ &+ y_{20}\{(y_7-y_2)y^c_5 + y^c_{24}y^c_{34}\} - {m_c}^2y_{35}y^c_{35}\Big)\,, \\ E_{4,1,1} &= \frac{4y_{16}}{x_1}(y_9\Big(y_{11}y_{32}y^c_{17} + ({m_b}^2y_{34} - y_{20}y^c_{24})y^c_{34}) \\ &+ {m_c}^2\{(y_2-y_7)y_{29}y_{31} + y_9(y_{35}y^c_{35} - y_{17}y^c_{17})\}\Big)\,, \\ E_{5,1,1} &= \frac{2y_1y_{16}y_{27}y_{29}}{x_1}\,, \\ E_{8,1,1} &= \frac{4}{x_1}\Big(y_9(y_{12}-y_{18})({m_b}^2y_{34} - y_{20}y^c_{24})y^c_{34} + 2q_{c1}\cdot k_1\langle q_0\cdot q'_{b1}\rangle\langle k_2\cdot k_1\rangle^*y_{27}y_{36}y^c_{35} + \\ &\quad {m_c}^2\{(y_2(y_{12}-y_{18}) - y_7y_{16})y_{29}y_{31} + y_9((y_{12}-y_{18})y_{35}y^c_{35} - y_{16}y_{19}y_{29})\}\Big) \qquad \text{(A10)} \\ E_{9,1,1} &= 0\,, \qquad \text{(A11)} \end{aligned}$$

where the index c means charge conjugation of the spinor, $|p_-\rangle = |p_+\rangle^c$.

APPENDIX B: POLARIZATION VECTOR FOR $B_c^*[1^3S_1]$ MESON

The expressions of the polarization vectors depend on the gauge choice. Here we choose a cartesian basis for the polarization vectors:

$$\epsilon^z(P) = \frac{1}{\sqrt{P_0^2 - P_z^2}}(P_z\,, 0\,, 0\,, P_0)\,, \tag{B1}$$

$$\epsilon^x(P) = \frac{|P_z|}{P_z M}\left(\frac{P_x P_0}{\sqrt{P_0^2 - P_y^2 - P_z^2}}\,, \sqrt{P_0^2 - P_y^2 - P_z^2}\,, \frac{P_x P_y}{\sqrt{P_0^2 - P_y^2 - P_z^2}}\,, \frac{P_x P_z}{\sqrt{P_0^2 - P_y^2 - P_z^2}}\right), \tag{B2}$$

$$\epsilon^y(P) = \left(\frac{P_y P_0}{\sqrt{P_0^2 - P_z^2}\sqrt{P_0^2 - P_y^2 - P_z^2}}, 0, \frac{\sqrt{P_0^2 - P_z^2}}{\sqrt{P_0^2 - P_y^2 - P_z^2}}, \frac{P_y P_z}{\sqrt{P_0^2 - P_z^2}\sqrt{P_0^2 - P_y^2 - P_z^2}}\right), \tag{B3}$$

which satisfy the conditions

$$\epsilon^i \cdot P = 0\,, \quad \epsilon^i \cdot \epsilon^j = -\delta^{ij}\,, \quad (i, j = x, y, z)\,. \tag{B4}$$

APPENDIX C: ROUTINES AND FUNCTIONS FOR THE HELICITY AMPLITUDE

In this Appendix, subroutines and functions for calculating the helicity amplitudes for the sub-process $gg \to B_c(B_c^*) + b + \bar{c}$ are explained.

SUBROUTINE BUNDHELICITY

Purpose: to compute the helicity amplitude of the bound state part, $\bar{b} + c \to B_c(B_c^*)$, where B_c is the lowest state of 1^1S_0 and B_c^* is the lowest one of 1^3S_1, with the expressions for the polarization as presented in appendix B.

Integer IBCSTATE=: state of the double heavy meson, IBCSTATE=1 for $B_c[1^1S_0]$; IBCSTATE=2 for $B_c^*[1^3S_1]$.

Real*8 BUNDAMP(4)=: four helicity amplitudes of the bound state part $c + \bar{b} \to B_c(B_c^*)$; BUNDAMP(4)=0 for $c + \bar{b} \to B_c$; BUNDAMP(4)=1 for $c + \bar{b} \to B_c$.

Real*8 POLAR(4,3)=: four Lorentz components of the three polarization vectors $\epsilon^k\,, (k = x, y, z)$ for the B_c^* state.

SUBROUTINE FREEHELICITY

Purpose: to compute the helicity amplitude of the process $gg \to \bar{b}+c+b+\bar{c}$. The functions M'_{Fm} $(m = 1, \cdots, 5)$, $E_{m,j,k}$ $(m = 1, \cdots, 9; j = 1, \cdots, 4; k = 1, \cdots, 64)$ are defined in the body of the paper.

Real*8 PMOMUP(5,8)=: the momenta PMOMUP(5,j) $(j = 1, \cdots, 8)$ in the process: PMOMUP(5,1) for the gluon-1, PMOMUP(5,2) for the gluon-2, PMOMUP(5,3) for the $B_c(B_c^*)$, PMOMUP(5,4) for the b, PMOMUP(5,5) for the $\bar{c}$, PMOMUP(5,6) for the $\bar{b}$, PMOMUP(5,7) for the c, PMOMUP(5,8) for the q_0 (the light-like reference momentum).

Real*8 PMOMZERO(5,8)=: eight light-like momenta obtained from PMOMUP(5,8) according to Eq.(29) respectively.

Real*8 COLMAT(5,64)=: $M'^{(\lambda_1,\lambda_2,\lambda_3,\lambda_4,\lambda_5,\lambda_6)}_{Fm}(\lambda_i = \pm,\ m = 1, \cdots, 5)$.

Integer IDP, IDQ0, IDB1, IDB2, IDC1, IDC2, IDK1, IDK2=: symbols (codes) for the particles in the processes: IDP for $B_c(B_c^*)$, IDQ0 for the reference massless fermion, IDB1 for b-quark, IDB2 for $\bar{b}$-quark, IDC1 for c-quark, IDC2 for $\bar{c}$-quark, IDK1 for gluon-1, IDK2 for gluon-2.

Complex*16 YUP(42)=: 42 possible non-zero spinor products $(y_i, i = 1, 2, \cdots, 42)$.

Complex*16 XUP(2)=: two possible double-spinor inner products (x_1, x_2).

Real*8 PROPUP(14,4)=: 14 possible denominators from the propagators appearing in the four basic groups of the Feynman diagrams (cb, bc, cc, bb).

Complex*16 BFUN(9,4,64)=: $E_{m,j,k}$ $(m = 1, 2, \cdots, 9; j = 1, \cdots, 4; k = 1, 2, \cdots, 64)$.

SUBROUTINE AMP2UP

Purpose: to compute the square of the helicity amplitude of the process $gg \to B_c(B_c^*)+b+\bar{c}$ by connecting the amplitude of the bound state part to that of the free quark part. The helicities of the intermediate quarks $c, \bar{b}$ are summed up, the whole amplitude is squared, and then all the 16 possible squared helicity amplitudes (if particle polarizations in the final state are not measured) are summed up. Here we also consider the three kinds of color flows explicitly.

Real*8 AMP2CF(3) =: three results of the square of the whole amplitude corresponding to the three kinds of color flows for the sub-process $gg \to B_c(B_c^*) + b + \bar{c}$.

Real*8 FINCOL(5,16) =: 16 possible helicity amplitudes for the process, where the helicities of the intermediate quarks have been summed up.

SUBROUTINE FIRST

Purpose: to compute the nine basic basic functions $E_{m,1,k}(m = 1, \cdots, 9; k = 1, 2, \cdots, 64)$. The correspondence of the nine functions to the Feynman diagrams is shown in Table II and Table III. In the present case: IDK1=1, IDK2=2, IDP=3, IDQ0=8, IDB1=4, IDB2=6, IDC1=7, IDC2=5.

SUBROUTINE SECOND

Purpose: to compute the nine basic functions, $E_{m,2,k}(m = 1, \cdots, 9; k = 1, \cdots, 64)$ obtained from $E_{m,1,k}$ by gluon exchange. Here IDK1=2, IDK2=1, IDP=3, IDQ0=8, IDB1=4, IDB2=6, IDC1=7, IDC2=5.

SUBROUTINE THIRD

Purpose: to compute the nine basic basic functions, $E_{m,3,k}(m = 1, \cdots, 9; k = 1, \cdots, 64)$ obtained from $E_{m,1,k}$ by b, c quark exchange and $\bar{b}, \bar{c}$ antiquark exchange. Here IDK1=1, IDK2=2, IDP=3, IDQ0=8, IDB1=7, IDB2=5, IDC1=4, IDC2=6.

SUBROUTINE FOURTH

Purpose: to compute the nine basic basic functions, $E_{m,4,k}(m = 1, \cdots, 9; k = 1, \cdots, 64)$ obtained from $E_{m,3,k}$ by gluon exchange. Here IDK1=2, IDK2=1, IDP=3, IDQ0=8, IDB1=7, IDB2=5, IDC1=4, IDC2=6.

FUNCTION DOTUP(I,J)

Purpose: to compute the dot-product of two momenta.

Integer I,J=: codes of the two particles.

FUNCTION INPUP(IP,JP)

Purpose: to compute the inner product of two spinors with light-like momenta based on the formula presented in APPENDIX A.

Integer IP, JP=: codes of the two particles.

FUNCTION SPPUP(IP,KP,JP)

Purpose(s): to calculate the spinor product with the formula presented in Appendix A.

Integer IP,JP,KP=: codes of the three particles.

FUNCTION POLSPPUP(I)

Purpose: to compute the spinor product involving the B_c^* meson polarization vectors with the formula presented in Appendix B.

Integer I=: one of the three polarization vectors for B_c^*.

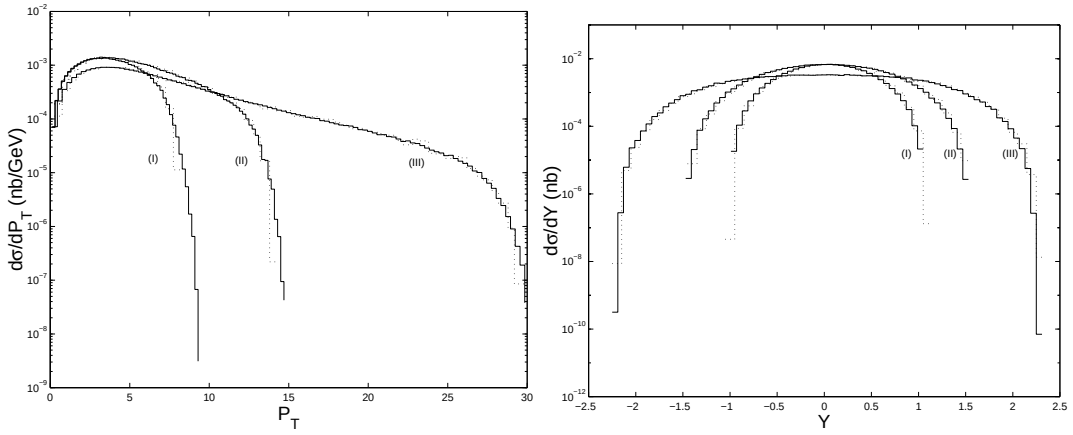

FIG. 9: B_c-$p_{\rm T}$ and B_c-Y(rapidity) distributions for the subprocess $gg \to B_c + b + \bar{c}$ with different center-of-mass energies $\sqrt{\hat{s}}$ =20 GeV(I), 30 GeV(II) and 60 GeV(III). The solid line shows the present results and the dotted line shows the results obtained in Ref.[7].

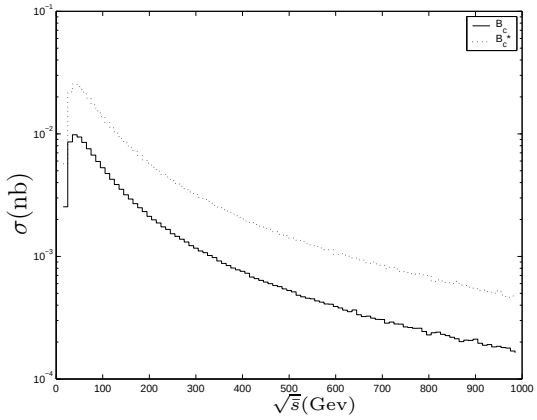

FIG. 10: Integrated cross sections for the subprocess $gg \to B_c(B_c^*) + b + \bar{c}$, with $\alpha_s = 0.2$, m_b = 4.9 GeV and $m_c = 1.5$ GeV. The solid (dotted) line corresponds to the B_c (B_c^*) production.

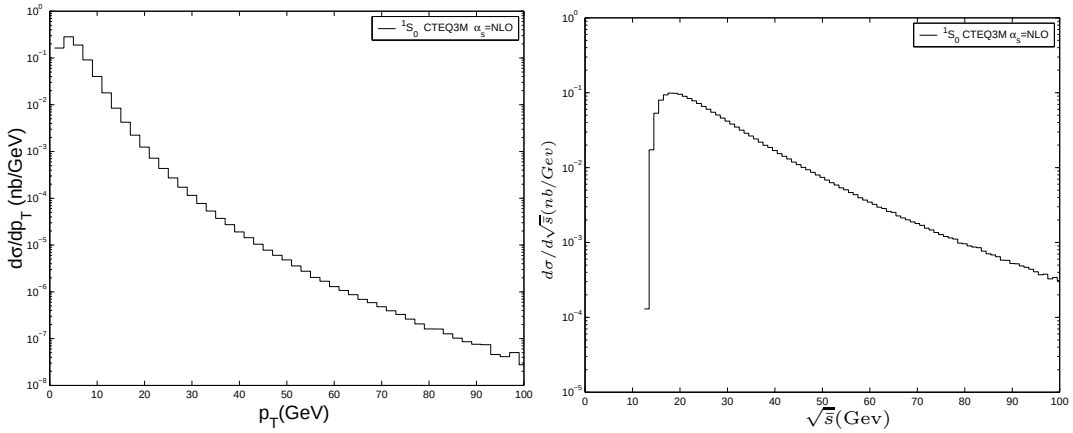

FIG. 11: B_c-$p_{\rm T}$ and $\sqrt{\bar{s}}$ distributions for the CTEQ3M parton distribution function by using α_s in the next-to-leading order (NLO) and adopting the characteristic energy scale squared $Q^2 = \bar{s}/4$, where $\bar{s}$ is the squared center-of-mass energy of the subprocess.

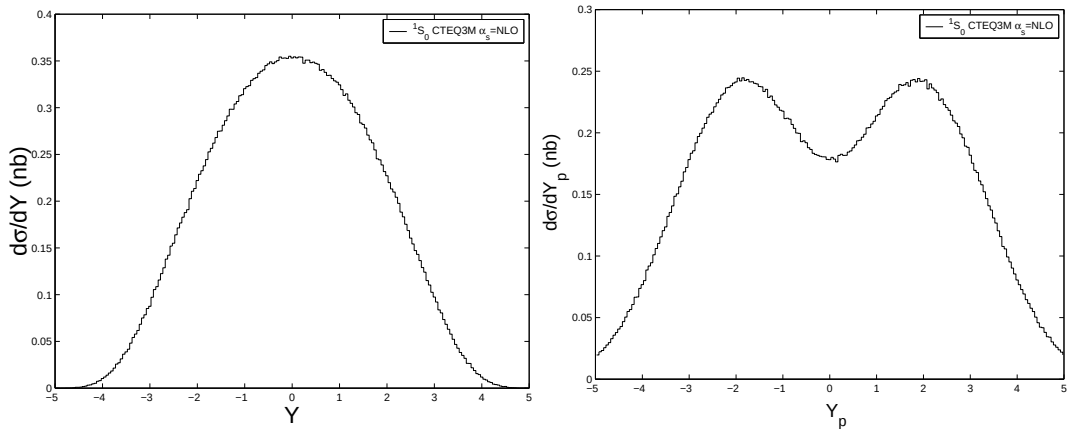

FIG. 12: B_c-Y (rapidity) and B_c-Y_p (pseudorapidity) distributions for the CTEQ3M parton distribution function, by using α_s in the next-to-leading order (NLO) and adopting the characteristic energy scale squared $Q^2 = \bar{s}/4$, where $\bar{s}$ is the center-of-mass energy of the subprocess.